UNCLASSIFIED

ORNL-1301(Del.)

Contract No. W-7405-eng-26

SOLID STATE DIVISION

QUARTERLY PROGRESS REPORT

for Period Ending May 10, 1952

D. S. Billington, Director

Edited by:

J. T. Howe

Photostat Price $ 9.30

Microfilm Price $ 3.60

Available from the
Office of Technical Services
Department of Commerce
Washington 25, D. C.

DATE ISSUED:

DEC 29 1952

OAK RIDGE NATIONAL LABORATORY
Operated by
CARBIDE AND CARBON CHEMICALS COMPANY
A Division of Union Carbide and Carbon Corporation
Post Office Box P
Oak Ridge, Tennessee

UNCLASSIFIED

UNCLASSIFIED

Quarterly reports previously issued in this series are as follows:

ORNL-1025	Period Ending January 31, 1951
ORNL-1095	Period Ending April 30, 1951
ORNL-1128	Period Ending July 31, 1951
ORNL-1214	Period Ending October 31, 1951
ORNL-1261	Period Ending January 31, 1952

167 002

PART I

CONTENTS

PART II

CONTENTS

467 004

SOLID STATE DIVISION QUARTERLY PROGRESS REPORT

INTRODUCTION

This report covers work performed in the Solid State Division for the quarter ending May 10, 1952. The following papers were presented by members of the division at a meeting of the American Physical Society held in Columbus, Ohio, March 20 to March 22:

R. H. Kernohan and G. M. McCammon, "Fading Characteristics of Gamma-Induced Coloration in High Density Glass," *Bull. Am. Phys. Soc.* 27, No. 2, 8 (1952).

J. H. Crawford, Jr. and J. W. Cleland, "Energy Levels in Ge Produced by Nucleon Bombardment," *ibid.*

R. E. Jamison and T. H. Blewitt, "Slip Lines in Pile Irradiated Copper Single Crystals," *ibid.*

R. R. Coltman and T. H. Blewitt, "The Effect of Neutron Irradiation on Metallic Diffusion," *Phys. Rev.* 88, 641 (1952).

W. E. Taylor, "Comparison of Thermally Induced Lattice Defects in Germanium and Silicon with Defects Produced by Nucleon Bombardment," *ibid.*, p. 642.

G. T. Murray and W. E. Taylor, "Neutron Bombardment of a Copper-Beryllium Alloy," *ibid.*, p. 642.

T. H. Blewitt, "Radiation Effects in Copper Single Crystals."

SUMMARY

RADIATION METALLURGY

Creep Under Irradiation. Work during this quarter has shown that irradiation can cause an increase or a decrease of creep in the same material, depending on the test conditions. To determine the cause of the wide discrepancy in creep information being reported by various laboratories, cantilever tests were run on type 347 stainless steel at temperatures between 1200 and 1400°F and at a maximum fiber stress of 8000 psi. It appears that for a given metal at a constant stress the effect of irradiation is to decrease the secondary creep rate at low temperatures and to increase the creep rate at higher temperatures.

Three in-pile tests of Inconel have been completed, and as it is now heat treated (1650 or 1700°F anneal), Inconel, with respect to its creep properties, is unstable under irradiation. The characteristics are typical of a metal undergoing metallurgical changes such as recrystallization during creep.

Extensometers. An extensometer utilizing a Bourdon tube and an electrical contact has been bench tested. The pressure-distention curve was linear to within ±0.0001 in. over 90% of the maximum travel. Further development and checking will be done with this type of gage before adapting it for use in the reactor.

Thermocouples. Stability tests have been run on chromel-alumel thermocouples in air at 1400 and 1500°F. A platinum-platinum-rhodium couple, calibrated against a National Bureau of Standards calibrated couple, was used as reference. Further stability tests will be conducted in helium and in vacuum.

In-pile thermocouple calibrations utilizing the melting point of sodium chloride were not run after it was found that the duration of the operating life of the quartz vessels that contained the salt was uncertain. Platinum tubing is being substituted for the quartz. Two-gram quantities of the copper-silicon eutectics are required to obtain good arrests in the cooling curve.

ENGINEERING PROPERTIES

ORNL Graphite Reactor Liquid-Metals Loop. An investigation into the cause of the flow stoppage that halted operation of the Inconel loop which circulated sodium through the graphite reactor showed that constrictions resulted from penetration at the welds. A gray, powdery material was found to have almost completely closed one joint in the colder part of the loop; x-ray examination indicates that the material is largely nickel.

A new loop was built with a modified surge tank to eliminate plugging at this point. During the bench testing period, a small leak developed in the electromagnetic pump cell, but it was closed by welding, and the loop was operated in the graphite reactor, hole 58N, for 6 hr at 1000°F and 95 hr at 1500°F before operation was halted by another leak in the pump cell. Specimens for examination have been cut from the external portion and will be cut from the portion that was in the reactor when the activity reaches a sufficiently low level.

Another loop with further improvements in weld joints and which incorporates a micrometallic filter bypass is being built. Tubing is being carefully inspected, and additional attention is being given to the elimination of oxygen from the sodium in the system. Improvements have also been made in the fabrication of electromagnetic flowmeter cells so that the final calibrated cells are more dependable in their operation than they were formerly.

LITR Sodium Stress-Corrosion Loop. The gaseous-displacement pump described in a previous quarterly report was found to be unsatisfactory when temperatures were raised to 1500°F because of solidification of sodium in the gas lines connecting the diaphragm chambers and the sodium-pump tanks. It was therefore decided to resort to the use of the more dependable electromagnetic type of pump, even though the advantages of incorporating the pump within the shield plug are lost. Approval for these modifications has been obtained from the Reactor Experiment Review Committee, and construction is in progress.

The pneumatic extensometer failed during bench testing at 1500°F. Further testing will be performed on slightly modified versions, but for the present experiments a Bourdon-tube extensometer will be adopted.

Measurement of Neutron Energy Spectra. Measurements of the neutron energy-spectra traverse of hole HB2 of the LITR are almost complete. These measurements will be correlated with future radiation-damage measurements. In order to obtain a broader coverage of energy and to check on previous data, three additional reactions are being investigated: $N^{14}(n,p)C^{14}$; $Cl^{35}(n,\alpha)P^{32}$; and U^{235} fission.

Nuclear Heating of Materials. Nuclear heating of materials will be measured in hole HB2 as a function of the position along the axis of the hole. A small calorimeter has been constructed that can be inserted in the 7/8-in. spiral tube that extends through the plug. Calibration may be accomplished by substitution of an electric heater for the specimen.

LIQUID FUELS

Radiation Damage to Liquid Fuels. Reactor fuels (Nos. 2, 3, and 17) in Inconel capsules have been exposed to irradiation at 1500°F, and chemical and metallurgical examinations have been made of the fuels and containers. Tests to date indicate that the beryllium salts (fuels Nos. 3 and 17) are not completely uniform after irradiation. If a beryllium salt is to be used as the reactor fuel, further investigation should be made.

Liquid-Fuels Irradiation in the MTR. Reactor fuel No. 21 in Inconel capsules will be tested in a 1 3/8-in.-dia hole in beryllium piece A-38 of the MTR to determine the effects of the higher flux on the fuel stability and corrosion properties at the operating temperature of 1500°F. The salt, which will be tested in a helium atmosphere, will generate approximately 3000 w/cc at a thermal flux of 4×10^{14}. It will therefore be necessary to dissipate heat from the capsule in order to maintain the operating temperature. Heat removal will be attained by air flow over the capsule and by process water flow over the outer assembly tube.

The capsule proposed for this test has been bench tested by using electric heaters to simulate a nuclear heating of 3500 w per cubic centimeter of capsule and an air flow of about 10 cfm at 30-psi inlet pressure to maintain the operating temperature of 1500°F. The assembly was then charged in beryllium piece C-48 of the LITR. To simulate the nuclear heating expected in the MTR a special UF_4-NaF salt was used that generated 1910 w/cc at a LITR power of 1000 kw. Another 140-hr irradiation was made at a power level of 1500 kw with a heat generation of 2450 w/cc. No difficulties were encountered in either run.

CRYSTAL PHYSICS

Y-12 Cyclotron Radiation-Damage Studies. Chemical and metallurgical analyses are given for proposed reactor fuels Nos. 2 and 14 after exposure at 815°C to proton bombardment in the 86-in. cyclotron. Several new types of targets were employed in an effort to increase the specific proton energy dissipated in the fuel. No radiation-induced corrosion was noted on the larger of the new style targets. With a "microcapsule" type of target, no indication of radiation-induced corrosion was found on runs of less

than 6 hours. After a 6-hr exposure at 815°C, metallographic examination showed a penetration of about 0.0025 in. greater than that of the control specimen. Energy dissipation based on the estimated irradiation volume rather than total volume of eutectic within the capsule was 4500 w/cc. Another irradiation, a duplicate run – except that the estimated energy was only 750 w/cc – showed no evidence of corrosion.

Thermal Conductivity of Structural Materials. During a 17-day irradiation period in the LITR, hole HB3, absolute thermal-conductivity measurements were made on a high-purity nickel specimen at temperatures of approximately 220, 300, 350, 430, 580, 700, and 800°C. No changes in conductivity as a function of irradiation time were found. These results are in agreement with relative conductivity measurements made in the ORNL graphite reactor.

Inconel specimens have been made for relative thermal-conductivity measurements in the ORNL graphite reactor and absolute conductivity measurements in the LITR. Although these experiments are not yet complete, measurements to date do not indicate a radiation-induced change in conductivity.

SPECIAL PROJECTS

Tests on Graphite-Uranium Oxide Bars. Graphite bars containing uranium oxide nodules in varying sizes and quantities were exposed in hole B of the ORNL graphite reactor for a period of one month. Pre- and post-irradiation measurements were made of weight, dynamic modulus of elasticity, electrical resistivity, and relative thermal conductivity. The thermal-conductivity measurements, which necessitated immersing one end of the specimen in a molten bath at 160°C, have apparently caused annealing in the control specimens but have not affected the uranium-bearing specimens. Further annealing experiments will be conducted.

Radiation Damage to Thorium and Beryllium. Dimensional and hardness measurements made on six thorium slugs irradiated for six months at Hanford indicated no significant changes in dimensions and only a slight hardness increase.

Dimensional measurements made on 14 beryllium bars irradiated for ten months at Hanford indicated no large change in dimensions, although lack of accuracy in preirradiation measurements made comparison difficult.

RADIATION METALLURGY

CREEP UNDER IRRADIATION

J. C. Wilson J. C. Zukas
W. W. Davis

From the work done this quarter it has been shown that under irradiation an increased or a decreased creep rate is possible in the same material, depending upon the test conditions. In addition, initial creep work on Inconel has indicated that under neutron bombardment this material is unstable metallurgically, to the detriment of its creep strength.

Tests on Type 347 Stainless Steel. It was previously reported[1] that the creep strength of metals decreased under irradiation; this was contrary to the findings of at least three other laboratories, Westinghouse Atomic Power Division,[2] North American Aviation,[3] and the NEPA Project.[4] Recently, however, Knolls Atomic Power Laboratory reported[5] results in agreement with the data of the ORNL group concerned with creep studies. Although several possible reasons for the disparity in the results of the various workers were discussed previously,[1] it was decided to run creep tests over a range of temperatures in an attempt to reconcile the oppositely held views. The tests were run on type 347 stainless steel, and experimental conditions were chosen intermediate between those heretofore employed at KAPL[5] and ORNL.[1] The test temperatures were between 1200 and 1400°F at a maximum fiber stress of 8000 psi in a cantilever apparatus.

The bench and in-pile tests were started at 1200°F and were subsequently raised to higher temperatures, as shown in Fig. 1 and in the tabulation of Fig. 2. The time-strain plot in Fig. 1 shows the form of the creep curves. The bench tests were run in duplicate, but the difference between the curves is so small that they are indistinguishable on a drawing of this scale. When plotted against the reciprocal of absolute temperature (Fig. 2), the minimum creep rates give a fairly straight-line relationship, except for the two highest temperature rates, for which the time of observation was very short. It may be seen that at 1200°F the ratio of the bench rate to the in-pile rate is 2.8, and it becomes unity at about 1400°F.

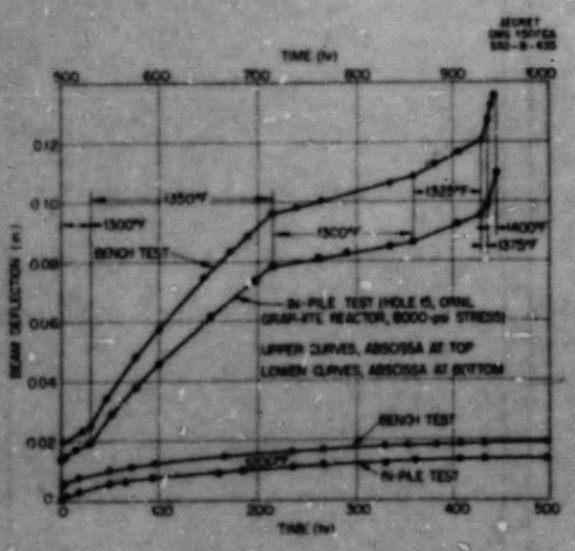

Fig. 1. Variable-Temperature Creep Test on Type 347 Stainless Steel; Beam Deflection vs. Time.

(1) J. C. Wilson, R. A. Weeks, J. C. Zukas, and W. W. Davis, *Physics of Solids Institute Quarterly Progress Report for Period Ending July 31, 1951*, ORNL-1128, p. 29.

(2) *Monthly Technical Progress Report; June 25, 1951 to July 25, 1951*, Westinghouse Atomic Power Division Naval Reactor Program, WAPD-NR-19, p. 29.

(3) E. P. Toohey, H. R. Jeppson, and R. D. Keen, *Effect of Cyclotron Irradiation on Creep of Aluminum*, NAA-SR-121 (June 8, 1951).

(4) C. E. Stilson, *In-pile Stress Deformation Tests*, NEPA-1817 (March 6, 1951).

(5) *Reactor Physics; Progress Report, May, June, July 1951*, Knolls Atomic Power Laboratory, KAPL-583, p. 71.

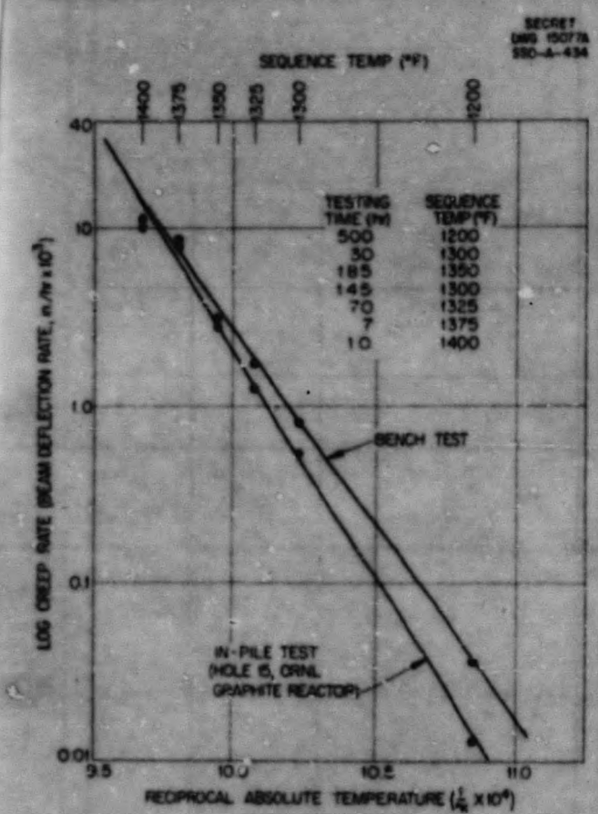

Fig. 2. Variable-Temperature Creep Test on Type 347 Stainless Steel; Log Creep Rate vs. Reciprocal Absolute Temperature.

By performing crude extrapolations of the data in Fig. 2 and by neglecting the effect of stress and flux, the following comparisons are made. Whereas KAPL[5] reports a much higher in-pile creep rate, by a factor of at least 7, these extrapolations indicate that the in-pile creep rate should be only one-fourth of the bench rate. If the earlier ORNL data of 1500°F and 1500 psi[1] are compared, it may be noted that the in-pile rate is greater than the bench rate by a factor of 2, in fair agreement with the extrapolated value of 1.5. Although the experimental results were not the same as those of KAPL,[5] in spite of similar experimental conditions, a basis for explaining the difference in the effects of bombardment reported by various observers was found. Apparently, for a given metal at a constant stress the effect of irradiation is to decrease the creep rate at low temperatures and to increase the creep rate at higher temperatures. The single test on nickel, reported last quarter,[7] substantiates this view. The temperatures at which irradiation has no effect on the creep rate (the point at which the curves of Fig. 2 cross) will probably be shifted by changes in stress or flux, and it is expected that this temperature will shift to higher values as the stress (and thus the strain rate) is increased. Should this shift occur as expected, it could account for the fact that the results on aluminum reported by both NAA[3] and NEPA[4] indicate decreased creep, although the temperatures employed were relatively high for aluminum.

Tests of Inconel. Upon completion of three in-pile tests of Inconel, it has been concluded that with respect to its creep properties Inconel as it is now heat treated (1650 or 1700°F anneal) is an unstable material under irradiation. If the concurrent bench and in-pile tests at 1500 psi and 1500°F shown in Fig. 3 are considered, the effect of neutron bombardment can be easily observed. The in-pile curves appear normal up to 50 to 100 hr of irradiation, at which time the creep rates increase rather sharply for a short period and then decrease slowly again. In the case of the upper curve (*A*), for the last 150 hr of the test the curve is linear, within the limits of experimental error. A second run (curve *B*) was made under the same conditions, except for a shorter time, to verify the form of curve *A*. The

[7] W. W. Davis, J. C. Wilson, and J. C. Zukas, *Solid State Division Quarterly Progress Report for Period Ending January 31, 1952*, ORNL-1261, p. 13.

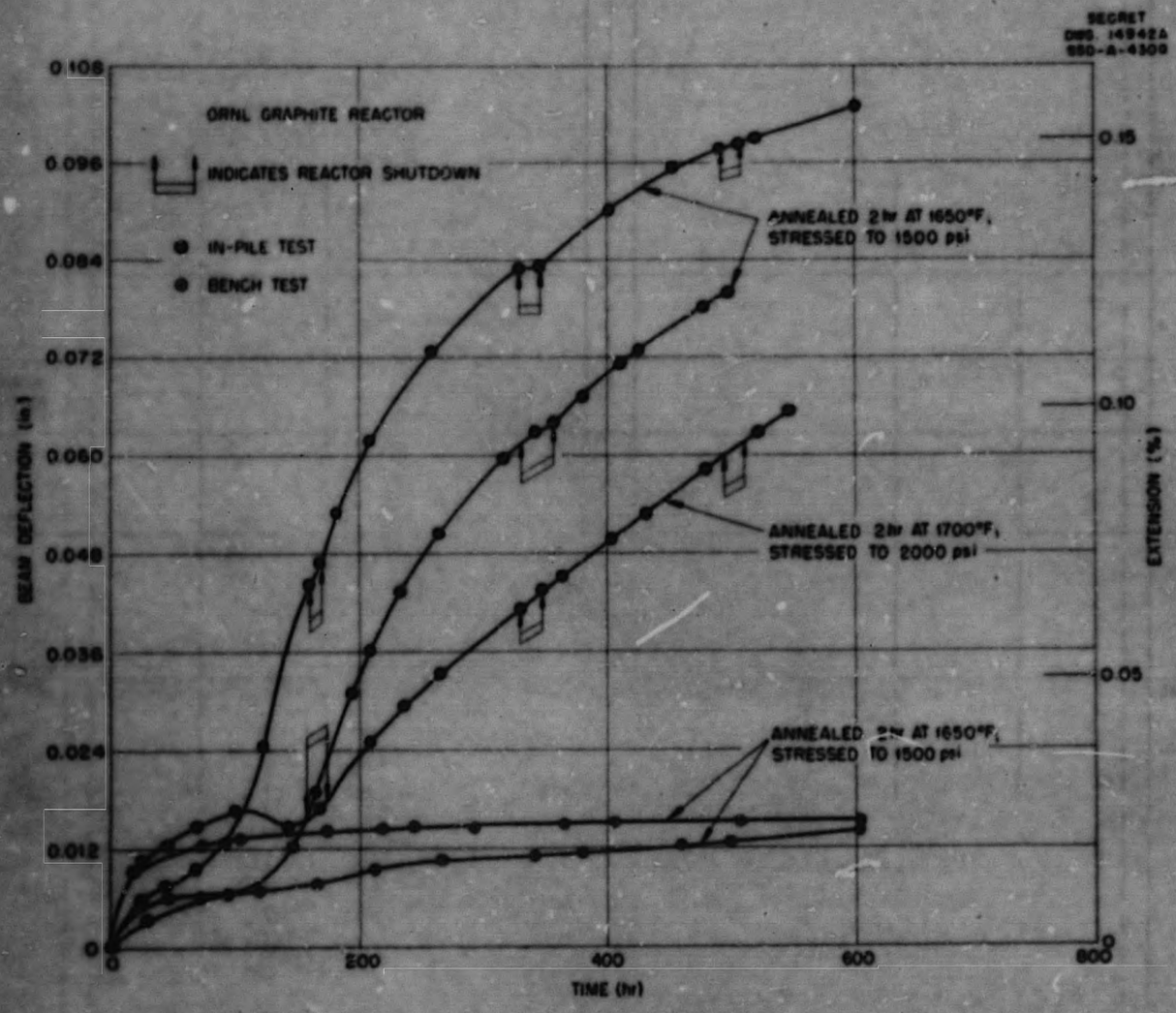

Fig. 3. Cantilever Creep Tests of Inconel at 1500°F.

creep rate for the second run decreased markedly during the reactor shutdowns between about 50 and 400 hr, but no such decrease was observed during the shutdown on the first run (*A*) at about 490 hours. The shape of these curves is typical of a metal undergoing metallurgical changes such as recrystallization during creep.[8] The bench tests (curves *D* and *E*, Fig. 3) were not particularly informative, except that the strain after 150 hr was less than the strain in the in-pile tests. At stresses below 3000 psi, creep tests of Inconel run in the Metallurgy Division have shown an upward inflection after periods of from 50 to 200 hours. At higher stresses and for prior anneals at temperatures of the order of 2000°F this phenomenon is absent. At first it was thought that the metallurgical change causing the large deformation was the carbide precipitation, but Skinner[9] of International Nickel

[8] J. N. Greenwood and H. E. Worcer, *J. Inst. Metals* 64, 135 (1939).

[9] Private communication, E. H. Skinner, International Nickel Company, to W. D. Manly, ORNL Metallurgy Division.

Company suggested that an order-disorder reaction takes place in Inconel. There is some indication that this is true in 80% nickel–20% chromium alloys,[10] although no x-ray evidence of a superlattice has been found. The scattering cross sections of nickel and chromium for neutrons are sufficiently different for neutron diffraction to be able to offer confirmatory evidence of a superlattice, and such an experiment is planned.

Figure 3 also gives the results (curve *C*) of a test in the reactor at a stress of 2000 psi. The annealing temperature (1700°F) was different from the foregoing tests (1650°F) because a change in the projected annealing temperature for materials was made during the interval between the experiments. Within the period between 90 and 150 hr of irradiation, this test exhibited abnormal behavior in registering "negative creep"; if these data are not valid, such an effect can be accounted for by postulating that the sign of the stress affects the over-all kinetics of whatever metallurgical change takes place. An actual homogeneous isotropic increase in the density of the specimen would give a curve such as *C* for a tensile creep test, but such a density change in the cantilever test would not be detected because of the geometry of the apparatus. No bench data at 2000 psi are yet available, and data at 1500 psi for times longer than those shown in Fig. 3 are not reliable because of a power outage and the failure of two microformers. Test *C* is still in the reactor and is operating at 1600°F.

A 1000-psi specimen is to be charged into the ORNL graphite reactor, and means will be provided for measuring the electrical resistance of the specimen during the test. A set of four Inconel creep specimens is being aged at 1500°F for 1000 hr in the unstressed condition, after which they will be tested to determine whether the anomalous in-pile behavior is caused by some metallurgical change that can be induced to occur before the start of the actual creep tests. Another apparatus operating at 1500°F and 1500 psi has been built and will be charged into the LITR to determine the effect of a higher flux.

The first model of a bellows-loaded tensile creep rig for the MTR has been designed, and shop construction has begun. The specimen is 1/2-in.-OD (0.035-in. wall) Inconel tubing from the same lot as is being used for corrosion testing in the Metallurgy Division. Several models of the furnace, which is placed inside the specimen, have been bench tested in an attempt to minimize temperature gradients.

EXTENSOMETERS

J. C. Wilson R. A. Weeks

It is believed that an extensometer utilizing a Bourdon tube and an electrical contact will be operable in the MTR because of its low mass (0.2 g), and that its simple geometry should simplify the problems of abstracting the heat generated in it by gamma-ray heating. Bench testing of this type of extensometer has begun, and Fig. 4 shows the bench-test setup. The tube was fabricated by filling a 0.060-in.-OD (0.005-in. wall) stainless steel tube with pulverized sodium chloride, roll flattening, bending, and then dissolving the salt in water. The tube is almost a complete circle, so its effective length with respect to thermal expansion is only about 1/8 inch. Sections of razor blades

[10] Z. Yano, *Japan Nickel Rev.* 9, 17 (Jan. 1941).

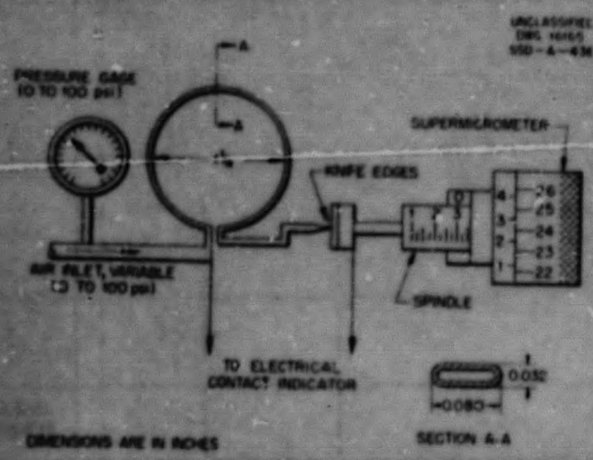

Fig. 4. Bourdon-Tube Extensometer.

were used as contacts. The distention was measured at various air pressures with an inexpensive 0- to 100-psi gage. The pressure-distention curve was linear to within ±0.0001 in. over 90% of the maximum travel (0.007 in. at 100 psig). Some hysteresis was noted, but this was attributed to the pressure gage, since the data were reproducible at the highest and lowest pressure points. Fixtures have been built to attach the unit to a recently received Templin calibrator that will permit measurement of distentions to approximately 0.00001 inch. A Baldwin pressure cell will permit pressure measurements to better than 1/4%, or 0.00002 in. in terms of movement of the tube. It is expected that more work will have to be done on the choice of contact elements; the temperature coefficient of the whole unit will also be determined by operation in an oven at temperatures up to 300°F.

A study will be made of the effects of neutron radiation on the static and emission characteristics of an RCA type 5734 transducer tube, which is in the can with the cantilever creep rig scheduled for charge in the LITR. Approximately 0.003-in. movement of the sensitive element of the tube gives a change in output voltage of about 40, and its low mass (1.7 g) should permit it to be used in high-flux reactors without excessive gamma-ray heating.

A piece of natural quartz 0.18 in. square and 1.3 in. long was irradiated in the LITR for a one-week period (7×10^{18} nvt) to determine whether irradiation produced dimensional changes, since the thermal expansion of quartz (along the *Z* axis) appears usable for calibrating extensometers in a reactor. A slight discoloration of the crystal was noted after irradiation, but, within the precision of measurement (0.05%), no dimensional changes were found. The specimen will be irradiated again.

THERMOCOUPLES

J. C. Wilson J. C. Zukas

Chromel-alumel thermocouples (30-gage) have been checked for stability in air at 1400 and 1500°F after two weeks and again after four weeks. The calibration shift was about 3 deg at the end of two weeks and 5 deg at the end of four weeks. The output voltage at constant temperature, referred to a platinum–platinum-rhodium thermocouple calibrated at the National Bureau of Standards, decreased with time; this is contrary to a report by Dahl[11] that the voltage should increase with time. The disparity was attributed to the difference in the depth of immersion of the couples in the aging and calibrating furnaces, and a new test has been started in which the thermocouples were aged and calibrated in the same furnace. At the end of 300 hr of a projected

(11) A. I. Dahl, "The Stability of Base-metal Thermocouples in Air from 800 to 2200°F," *Temperature, Its Measurement and Control in Science and Industry*, American Institute of Physics, p. 1230, Reinhold, New York, 1941.

2000-hr test, the three sizes of thermocouples (20-, 24-, and 30-gage) are showing increases in output voltage proportional to time and wire gage, in qualitative agreement with Dahl. An apparatus to perform the same test in helium and in vacuum has been designed.

In-pile thermocouple calibrations utilizing the melting point of sodium chloride had been planned, with fused quartz as the container material. However, the duration of the operating life of such containers has been erratic, and new containers of 1/8-in. platinum tubing have been fabricated by the Research Shops. Testing of these units has started. As an alternate for sodium chloride, copper-silicon alloys have been tested in fused quartz, but samples weighing 2 g were required for good arrests in the cooling curve. Copper-silicon eutectics and the minimum-melting-point alloy of copper and manganese are being made in the Metallurgy Division for further melting-point studies. In developing the apparatus, weights and heat losses are balanced so that the gamma heating in the MTR will not affect the operation.

RADIATION DAMAGE TO ELECTRONIC EQUIPMENT

R. A. Weeks

An investigation of the effects of radiation on complete units of electronic equipment has been initiated. Earlier work[12] has shown that the d-c and low-frequency characteristics of a majority of conventional electronic components are affected only slightly, if at all, by an exposure of 10^{15} (or greater) nvt.

In order to speed up testing of other components and to test further the previously irradiated components under a greater variety of conditions, irradiation of complete sets of equipment is thought to offer many advantages. Testing of the operating unit subjects all components to widely varying conditions of frequency, voltage, current, and temperature. The testing of the individual components under such a wide range of conditions would be difficult and uneconomical.

These tests will be made under the aegis of the Solid State Division, which is interested in obtaining information on the behavior of high-frequency components being considered for use in transducer circuits for in-pile tests.

The Bulk Shielding Facility is being used for these tests. In order to use this reactor, a tank was built large enough to accommodate the largest unit to be tested. The tank may be depressurized to simulate high altitude, and 100 test or power leads and ten coaxial leads have been provided to furnish power to the unit under test and to provide test points for dynamic electrical testing of components of the unit. The tank has two Plexiglas windows in the top.

Immersion testing of the tank has been completed, and the irradiation of the first unit, a low- and medium-frequency radio compass has begun. The radio compass receiver and its loop antenna are being irradiated. The loop antenna is placed in a shielded box that contains a signal antenna excited by an external signal generator.

(12) E. R. Child and H. J. Harpole, *Effects of Fission Produced Radiation on Electronic Equipment*, Engineering-Physics Division, Frederick Flader, Inc., NEPA- , (Jan. 31, 1948).

The tank has been placed in the Bulk Shielding Facility so that the thermal flux at the point in the tank nearest the reactor is approximately 8×10^8 neutrons/cm^2·sec, the fast flux is approximately 10^8 neutrons/cm^2·sec, and the gamma flux is approximately 10^{11} 1-Mev gamma photons/cm^2·sec.[13] Operations will be for a minimum of 100 hr at these levels. At some future date measurements will be made on the flux distribution in the tank.

No progress has been made on the measurement of radiation effects on cables and dielectrics,[14] because the dielectrometer has not yet been received from the Bureau of Ships. Delivery of this equipment is expected in June.

[13] H. E. Hungerford, *Bulk Shielding Facility Water Data Work Sheet*, ORNL CF-52-2-37 (Feb. 1, 1952).

[14] R. A. Weeks, *op. cit.*, ORNL-1261, p. 19.

ENGINEERING PROPERTIES

ORNL GRAPHITE REACTOR LIQUID-METALS LOOP

C. D. Baumann
R. M. Carroll
C. Ellis
D. T. James
M. T. Morgan
O. Sisman
W. W. Parkinson

The in-pile portion of the Inconel loop containing sodium, which had operated for two weeks in the ORNL graphite reactor,[1] was removed from the reactor shield and taken to the burial ground. After the activity of the loop had dropped sufficiently for safe handling, specimens were cut from both the in-pile and the external portions for metallographic examination. In an investigation of the cause of the flow stoppage that had halted operation, constrictions that resulted from penetration at the welds were found in the tubes. One of these constrictions, in the colder part of the loop (the junction of one tube with the surge tank), was almost completely closed by gray, powdery material. X-ray examination indicated that the powder was largely nickel. The powder is now being analyzed spectrographically.

Another sodium-loop system was constructed that used 19-ft one-piece tubular heaters that were made to order and a modified surge tank designed to avoid plugging. The arrangement of tubing, surge tank, electromagnetic flowmeter, and pump is shown in Fig. 5. At the conclusion of the bench test on the loop, a very small leak was found in the pump cell; however, the leak was successfully closed by welding, and after further bench testing, the loop was installed in the reactor. Figure 6 shows the loop and associated equipment in place in the reactor. The apparatus as shown is typical of all liquid-metal loops built to date. The loop operated for 6 hr at 1000°F and 95 hr at 1500°F, after which the operation was halted because of a small leak, which occurred again in the pump cell. The presence of the sodium leak was indicated by an activity monitor located on the air suction line from the shield compartment around the external portion of the loop. After two weeks of decay of the sodium activity, the external portion of the loop was cut off and the remainder of the loop was pulled into the shielding. Specimens have been cut from the external portion and will be taken from the part of the loop that was in the reactor as soon as it decays to a safe level.

[1] C. D. Baumann, R. M. Carroll, C. Ellis, D. T. James, M. T. Morgan, O. Sisman, and W. W. Parkinson, *Solid State Division Quarterly Progress Report for Period Ending January 31, 1952*, ORNL-1261, p. 21.

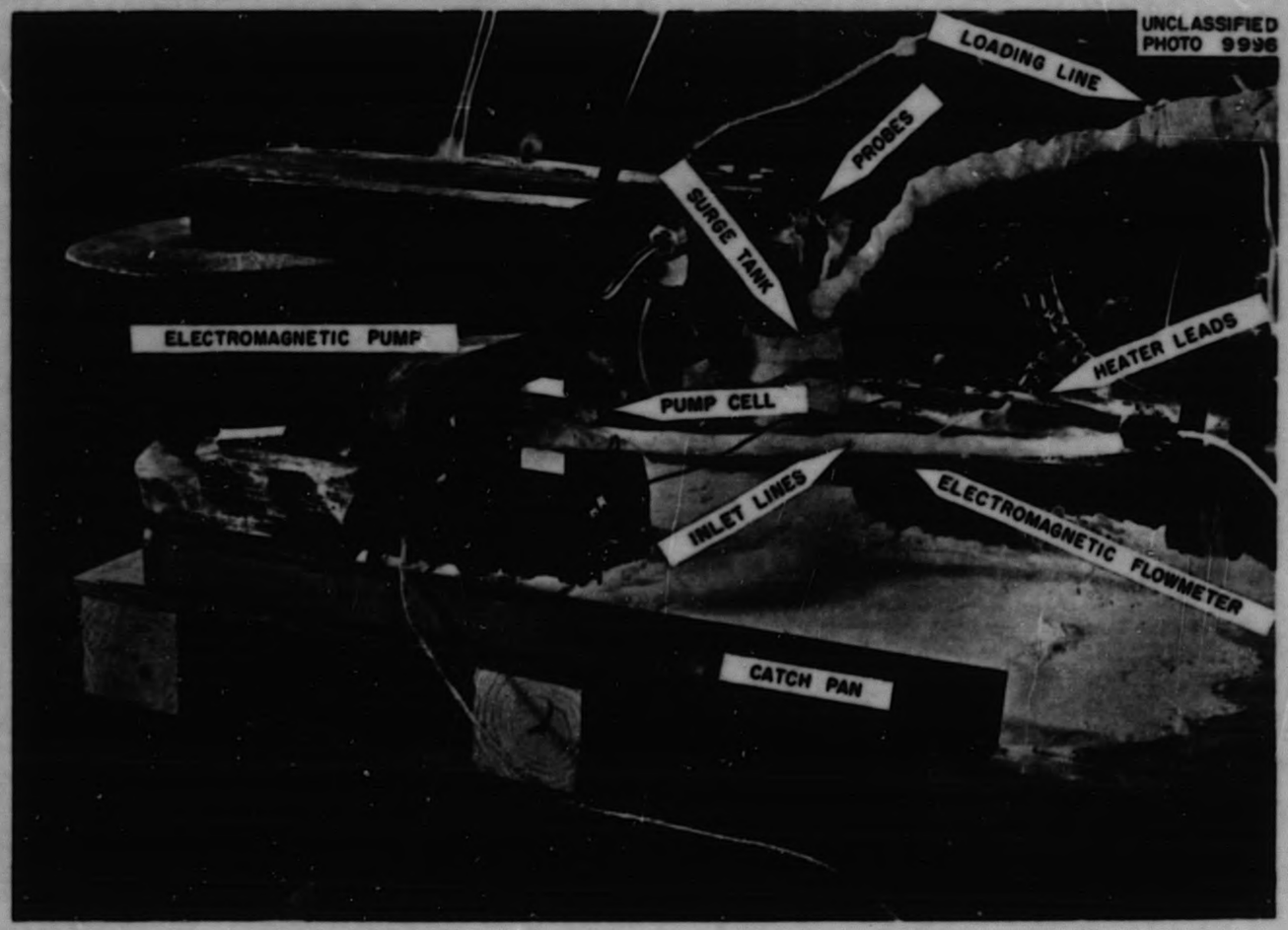

Fig. 5. Sodium-Loop System, Bench-Test Setup.

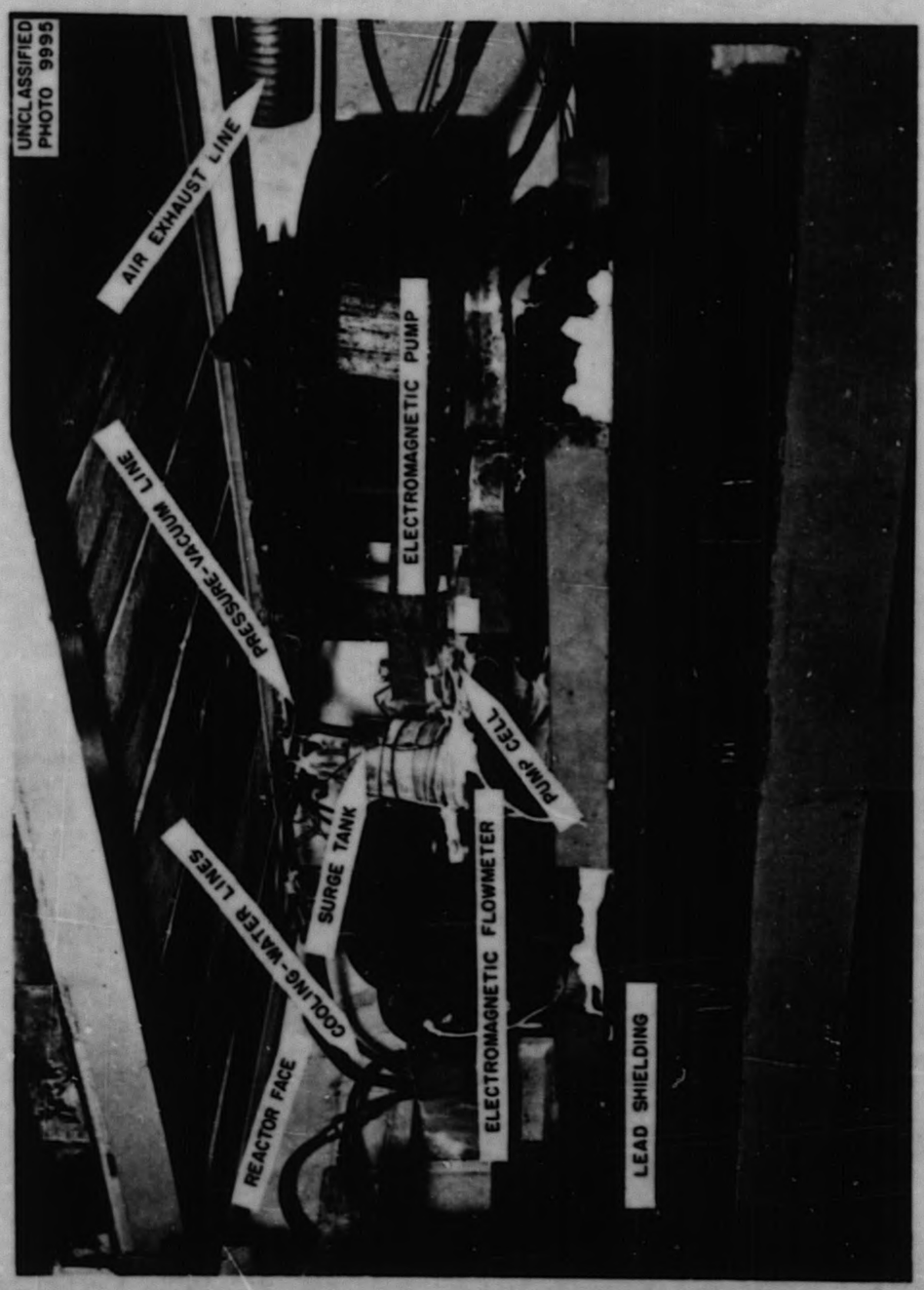

Fig. 6. Sodium-Loop System, In-Pile Setup.

To eliminate the constrictions at welded joints, a method of butt welding the tubes by means of ferrule connections has been developed. Another loop utilizing this method of fabrication and incorporating a micrometallic filter bypass is being built. The filter and a cooling tank are being added in a partial bypass of the in-pile part of the loop to remove sodium oxide and insoluble material in the circulating sodium.

To avoid the recurrence of leaks, an extensive testing program on materials and fabricated parts has been initiated. Tubing is being examined by means of x rays and fluorescent penetrant oil, and assembled parts are being examined by these methods when applicable, as well as being leak-tested under both pressure and vacuum.

Since oxygen contamination of the sodium may be responsible for corrosion, mass transfer, and obstruction of the tubing, changes have been made in auxiliary equipment to eliminate all traces of oxygen from the sodium in the loops. A new filling system has been assembled with additional filters in the lines. Another useful feature of this system is a metering tank having a screw-driven electric probe operating through a rubber stopper to indicate sodium level. The filling apparatus is shown in Fig. 7. Another remedial measure was the installation of a purifier in the helium apparatus that supplies the atmosphere over the loop surge tank. This purifier is a sodium-potassium bubbler (cf. "LITR Sodium Stress-Corrosion Loop" and Fig. 9, this report).

The electromagnetic flowmeter cells on previous liquid-metal loops have given various difficulties, most of which were traceable to the attachment of the lead wires. These difficulties have been eliminated in the development of a standard type of flowmeter

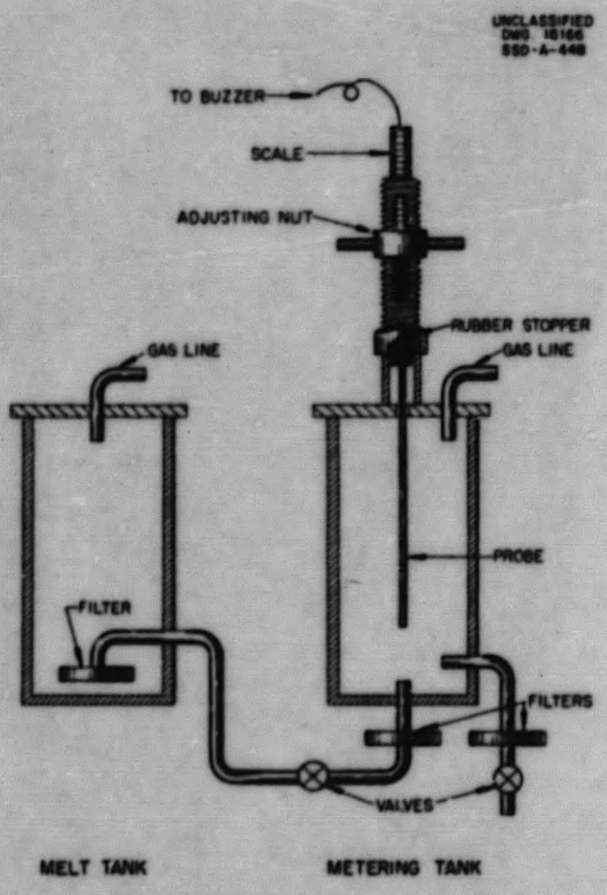

Fig. 7. Molten-Sodium Metering Tank.

cell, and two sizes of this type in both Inconel and type 316 stainless steel are being calibrated. These cells consist of a 3-in. length of tubing through which a hole has been precision-drilled along the diameter at right angles to the axis of the tube. A wire of the same material as the tube is inserted through the hole and brazed in with nickel-palladium filler. The portion of the wire through the bore of the tube is then drilled out flush with the inner wall of the tube.

The flowmeter cells in the calibration apparatus were connected end to end, with the lead wires in the same plane, between two tanks of known volume with level-indicating electrical probes. Sodium could be

forced through the flowmeter cells at a controlled rate by pressurizing or evacuating these tanks. A high-flux magnet of measured field strength was fixed around each cell in turn and the output voltage was recorded on a Brown recorder. These improved calibrated cells should remove the uncertainties from flowmeter operation.

LITR SODIUM STRESS-CORROSION LOOP

W. E. Brundage
R. M. Carroll
C. Ellis
A. S. Olson
W. W. Parkinson

The design, fabrication of parts, and operating tests of an apparatus for circulating molten sodium through a stress-corrosion specimen in the LITR have been described in the two previous quarterly reports.[2,3] To simplify the problem of shielding, the apparatus was designed so that all parts containing sodium could be placed in a beam hole of the reactor to utilize the reactor shield. Space limitations required the development of a special pump, and a bench model of a gaseous-displacement pump designed for this purpose has been under test for some time.[3]

The operating temperature of the gaseous-displacement pump was increased from 1000 to 1500°F to check its operation with sodium at high temperatures. It was impossible to operate longer than 4 to 6 hr at this temperature because of condensation and freezing of sodium in the gas lines connecting the diaphragm chambers and the sodium-pump tanks. The sodium vapor was carried through the vapor traps and into the lines by the pumping gas as it was being displaced into a diaphragm chamber. The use of larger connecting tubes extended the operating time, but eventually these, too, were blocked to the point of uselessness. After these periods of intermittent operation it became apparent that one of the check valves was not operating satisfactorily. This allowed all the sodium to be forced into one tank, and the surge of displacing gas blew liquid sodium into one of the connecting lines, where it was quickly frozen. To find the cause of check-valve failure the pump was disassembled, and the check valves were cut open. One of the valve seats proved to be badly scored. Since all the valves had operated satisfactorily earlier, the scoring was probably not an effect of operation, but rather due to faulty construction.

A new pump-and-loop system was constructed of Inconel with two check valves in series substituted for each of the single valves of the earlier arrangement. An additional change in the system was to alter the diaphragm chambers to give the diaphragms a stroke displacing a fixed volume of gas. This fixed-volume displacement for each half of a pumping cycle would allow the sodium level in the pump tanks to reach an equilibrium position in case of unequal flow resistances on the two halves of a cycle. This attainment of an equilibrium condition should prevent collection of all the sodium in one tank with subsequent "blowing over" of the displacing gas. The pumping cycle was also changed from 30 to 10 sec to transfer less sodium from one tank to the other during a cycle, thereby reducing the probability that a tank would be completely emptied in one cycle. The system operated satisfactorily with alcohol for a 3-hr period and was then filled with a measured quantity of filtered sodium. Vapor condensation continued to obstruct the connecting

[2] A. S. Olson, W. E. Brundage, W. W. Parkinson, and O. Sisman, *Physics of Solids Institute Quarterly Progress Report for Period Ending October 31, 1951*, ORNL-1214, p. 32.

[3] W. E. Brundage, R. M. Carroll, C. Ellis, A. S. Olson, O. Sisman, and W. W. Parkinson, *op. cit.*, ORNL-1261, p. 21.

tubes in spite of the use of an improved vapor trap. The experiment was terminated when a split developed in the Inconel tubing (see Fig. 8) and caused a small sodium leak and fire.

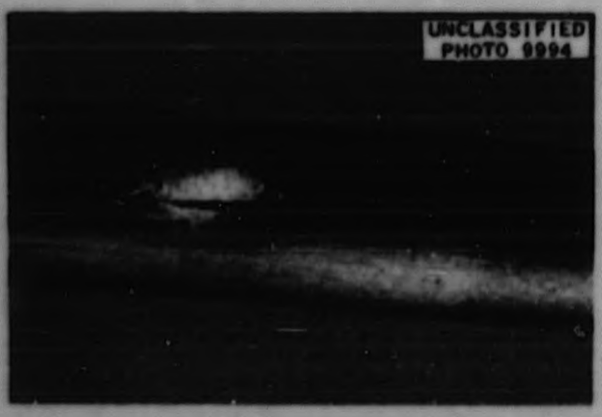

Fig. 8. Ruptured Inconel Tubing in Sodium-Loop System.

The difficulties arising from vapor condensation in the gas lines of the gaseous-displacement pump make it advisable to replace this type of pump with the more conventional a-c electromagnetic type. The size of an electromagnetic pump prevents its being placed inside the beam hole in the reactor shield as had been planned for the system using the gaseous-displacement pump. Alterations of the design of the equipment, which were required by this change in location of the pump, have been made. The sodium tanks of the displacement pump can be utilized as surge tanks for the electromagnetic pump, the major charge required being the addition of connecting tubing through the shield plug to circulate sodium from the pump through the specimen section of the system. These connecting tubes must be traced by electric heaters for melting the sodium prior to startup, and measurement of temperatures by use of thermocouples at various points along these tubes is desirable. The controls for the heaters and a temperature recorder can be added to the present control panel, since the replacement of the gaseous-displacement pump permits omission of its pressurizing controls. Minor changes must also be made in the alarm and safety circuits of the reactor instrumentation.

Portions of the system that will contain radioactive sodium outside the reactor shield will require the construction of a suitable shield and support. Calculations indicate that a lead shield approximately 8 in. thick will be needed, and if the dimensions of the exterior system are kept to a minimum, this will amount to about 9000 pounds. The external parts of the sodium system, including the electromagnetic pump and flowmeter, will be enclosed for reasons of safety in a metal box filled with helium. These modifications and additions to the apparatus have been approved by the Reactor Experiment Review Committee.

Nickel-palladium brazing has been used to assemble parts of the sodium system attached to the stressed specimen, and fabrication of the unaltered parts of the apparatus is about 90% complete. Alterations and fabrication of equipment involved in the changes incident to the use of an external pump are about 25% complete.

The latest model of the pneumatic extensometer,[3] which is to be attached to the stressed specimen to provide creep data, failed during testing at 1500°F owing to galling. A slightly modified version that was held to much closer machining tolerances has been received from the shops and is being set up for testing at the operating temperature. If galling or seizing of the extensometer were to occur during a stress-corrosion experiment, the extensometer would absorb some of the load from the specimen and invalidate the stress-corrosion

measurements. To eliminate this possibility, a Bourdon-tube extensometer, described by Wilson and Weeks (cf. "Extensometers," this report), is being constructed of Inconel to withstand high temperatures and to eliminate thermal expansion corrections when used with Inconel specimens.

The helium purifiers[3] that provide an inert atmosphere for the space around the Inconel specimen and tubing have been completed. The scrubber towers have been filled with pyrex helical column packing and sodium-potassium eutectic, and one unit has been placed in operation on the ORNL graphite reactor sodium loop (Fig. 9).

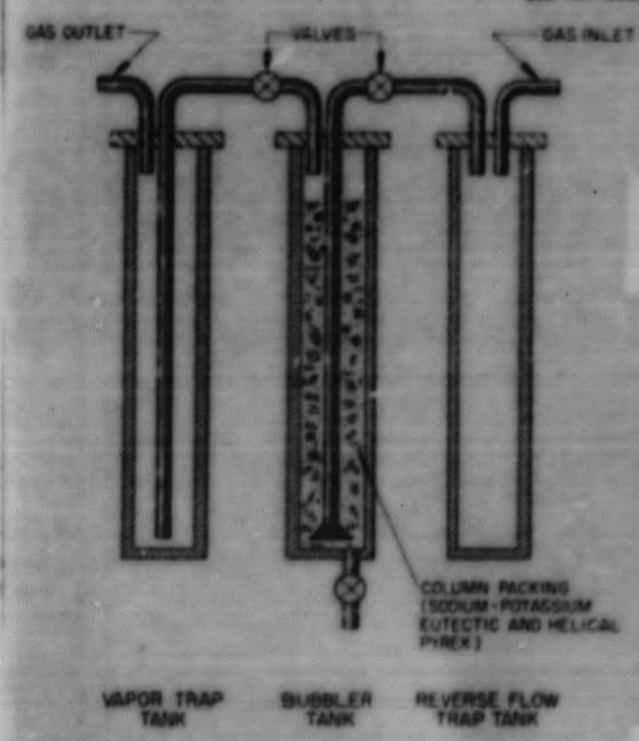

Fig. 9. Helium Purification System.

MEASUREMENT OF NEUTRON ENERGY SPECTRA

J. B. Trice D. T. James

A series of measurements to determine the neutron energy spectrum as a function of position in the LITR, hole HB2, is almost completed. The results of these measurements will be used for future correlation with the results of radiation-damage tests to be made in this hole and will also be valuable in determining the flux and flux spectrum as a function of distance from the active lattice.

The method for determining the neutron energy spectrum is that reported in the last quarterly report.[4] For the present tests, however, more measurements are being made in order to map the neutron energy spectra as a function of position along the longitudinal axis of the HB2 hole. A distance of about one linear foot along the axis and adjacent to the reactor plate is being mapped. In addition to the ten nuclear reactions used in the previous test, at least three additional ones are being investigated. These include $N^{14}(n,p)C^{14}$, $Cl^{35}(n,\alpha)P^{32}$, and U^{238} fission.

The cross section for the reaction $N^{14}(n,p)C^{14}$ has strong resonances at 0.65 and 1.42 Mev, which is the energy region where previous reactions have yielded little information. This, together with the long life of C^{14}, may permit the reaction to be very useful for measuring the total integrated fast flux in a critical energy region.

---

[4] J. B. Trice, *op. cit.*, ORNL-1261, p. 26.

The U^{238} fission reaction, with an effective threshold of about 1 Mev, will be used as a check on spectra data already existing. This will be done by first calculating the quantity

$$\int_0^\infty \phi(E)\,\sigma_f(E)\,dE \ ,$$

by using the measured neutron spectrum $\phi(E)$ integrated over the fission cross section, and then by measuring this integrated quantity by the fission of U^{238}. Agreement of these two quantities would indicate that the spectrum as measured was probably correct within the limits of known experimental errors. The U^{238} fission reaction will be used in a similar way to the $N^{14}(n,p)C^{14}$ reaction to serve as a check on an already measured spectrum, since the fission cross section is known accurately.

The reaction $Cl^{35}(n,\alpha)P^{32}$ is possible from the standpoint of energy for neutrons having a minimum energy of 0.96 Mev. The effective cross section for this reaction for high-energy reactor neutrons is being determined from irradiation of NaCl during the present tests. As more information is obtained about this reaction, it can probably be included with the others that have already been proved reliable for measuring neutron spectra.

Most of the reactions used for these measurements yield radioactive materials that are easily measured by either a high-pressure ionization chamber that is sensitive to gammas only or by a standard beta counter. The $N^{14}(n,p)C^{14}$ and $U^{238}(n,f)FP$ reactions, however, require special techniques. For the $N^{14}(n,p)C^{14}$ reaction, it is necessary to use a beta counter to which CO_2 gas containing the C^{14} is admitted. The betas, which are very soft, ionize the CO_2 gas and are then easily measured. Such a counter is calibrated with a standard sample of CO_2 labeled with C^{14}. For the U^{238} fission reaction, special care will have to be exercised in fixing the irradiation time because of the presence of fission products with different activities and half lives. The use of a simple exponential relationship for decay rates is therefore impossible, and it will be necessary to compare the activity from the test sample of U^{238} with the fission activity from a sample of U^{235} irradiated in a known flux of thermal neutrons. Both samples will be irradiated for the same period of time and will also be counted at the same time.

During the period of collecting the data from fast-neutron reactions, it was necessary to monitor the thermal-neutron flux constantly. Table 1 shows a compilation of all thermal-neutron flux measurements taken in hole HB2 of the LITR. The date and reactor power are included as reported by the Reactor Operations Department. Figure 10 shows two curves giving $(nv)_{th}$ as a function of position along the longitudinal axis of the hole for two different reactor power levels, 850 and 1000 kw. The zero position along the horizontal axis coincides with the end of hole HB2 adjacent to the active lattice and separated from it by a 1/4-in.-thick aluminum plate.

NUCLEAR HEATING OF MATERIALS

J. B. Trice D. T. James

A calorimeter for measuring the nuclear heating produced in various

materials was designed and constructed. It is smaller than those previously used and is thus adapted for measurements at positions that are less accessible. For example, it is planned to measure the nuclear heating produced in various materials placed in hole HB2 of the LITR by inserting the calorimeter into a 7/8-in.-ID spiral tube that extends through a series of three shield plugs to the aluminum plate adjacent to the active lattice. The heating rate as a function of position along the axis of HB2 will be determined from the emf's of two copper-constantan thermocouples fastened inside the calorimeter. Calibration of the calorimeter is accomplished by substituting an electric heater for the specimen to be irradiated. Thermocouple response as a function of heater power is then recorded and expressed graphically for use in actual measurements during reactor irradiation of specimens.

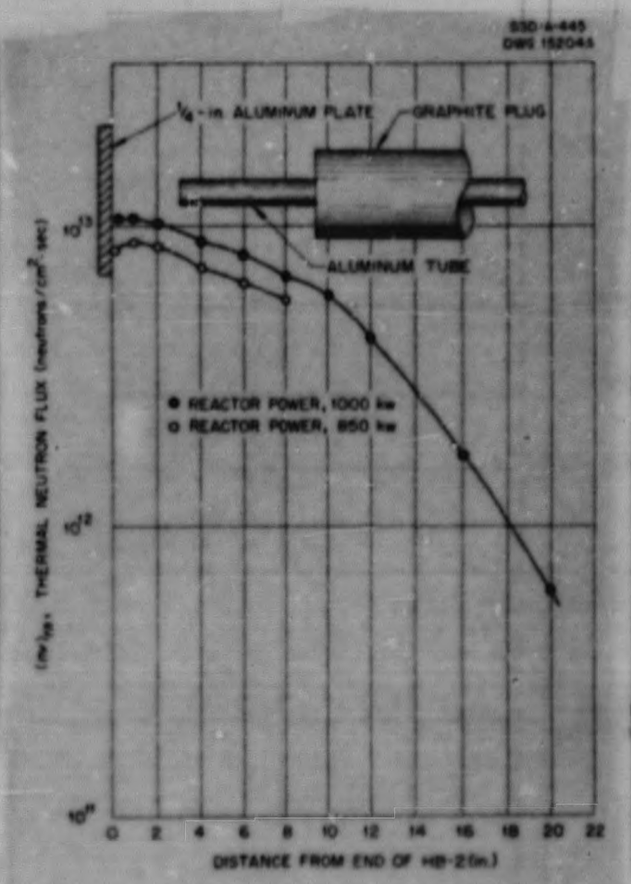

Fig. 10. Thermal-Neutron Flux Traverse in LITR, HB-2.

Table 1

THERMAL-NEUTRON FLUX AS A FUNCTION OF DISTANCE FROM REACTOR END OF HOLE HB2

DISTANCE FROM REACTOR END OF HB2 (in.)	THERMAL FLUX, $(nv)_{th} \times 10^{-13}$	
	1.00-megawatt Reactor Power*	0.85-megawatt Reactor Power**
0.25	1.163	0.908
1.00	1.163	0.964
2.00	1.106	0.926
4.00	0.973	0.794
6.00	0.879	0.700
8.00	0.740	0.605
10.00	0.626	
12.00	0.456	
16.00	0.1757	
20.00	0.606	

*April 2, 1952.
**April 16, 1952.

SPECIAL PROJECTS

TESTS ON GRAPHITE-URANIUM OXIDE BARS

R. H. Kernohan

Postirradiation measurements have been made on the graphite-uranium oxide bars discussed in the previous quarterly report.[1]

All test specimens were molded resin-bonded bodies made with a 5% uranium metal composition (added as UO_2) by weight; the UO_2 particles occupied about 3% of the volume. In preparation the specimens were baked at 2500°F (1370°C) and were not graphitized.

Four batches of bars, each with different UO_2 particle sizes, were made that contained UO_2 with 93% U^{235} enrichment. Another four batches were made that contained UO_2 with normal uranium (0.7% enrichment). Several control test bars containing no uranium were also fabricated. Batch designations and descriptions are explained in Table 7.

Each specimen, approximately 0.230 by 0.296 by 2.86 in. in size and weighing about 5.5 g, was weighed accurately before and after irradiation. The enriched UO_2 bars (S, T, U, V) averaged 1.75 in specific gravity, and the normal UO_2 bars (X, 2X, 3X, 4X) averaged 1.71. The control bars (R) averaged 1.66 in specific gravity. In addition to the determination of weight, tests were made on the dynamic modulus of elasticity, electrical resistivity, and relative thermal

(1) R. H. Kernohan, *Solid State Division Quarterly Progress Report for Period Ending January 31, 1952*, ORNL-1261, p. 41.

Table 7

DESCRIPTION OF GRAPHITE-URANIUM OXIDE BARS

BATCH LETTER	DESCRIPTION OF URANIUM ADDITION
R	No uranium
S	Enriched uranium nodules, -35 + 40 mesh U.S. standard; average particle size, 586 ± 16 μ (microscopically determined)
T	Enriched uranium nodules, -50 + 70 mesh; average particle size, 334 ± 7 μ (microscopically determined)
U	Enriched uranium nodules, -140 + 325 mesh; average particle size, 94 ± 0.2 μ (microscopically determined)
V	Enriched uranium nodules, -325 mesh; particle size < 44 μ (estimated)
X	Normal uranium nodules, -35 + 40 mesh (same as batch S)
2X	Normal uranium nodules, -50 + 70 mesh (same as batch T)
3X	Normal uranium nodules, -140 + 325 mesh (same as batch U)
4X	Normal uranium nodules, -325 mesh (same as batch V)
Z	AGOT graphite cut parallel to extrusion direction
2Z	AGOT graphite cut perpendicular to extrusion direction

Table 8

RADIATION HISTORY OF GRAPHITE-URANIUM OXIDE BARS

CONTAINER	DATES OF IRRADIATION	FLUX (nv)	REACTOR-ON TIME (hr)	INTEGRATED FLUX (nvt)	INCREMENT OF REACTOR POWER (kwhr)	HIGHEST TEMPERATURE ATTAINED (°C)
A	12/12/51 to 1/7/52	9.3×10^{11}	567.8	1.90×10^{19}	2,176,534	86
B	1/7/52 to 2/4/52	8.6×10^{11}	582.6	1.80×10^{19}	2,199,567	66
C	2/4/52 to 3/3/52	8.3×10^{11}	613.8	1.83×10^{19}	2,248,238	88

conductivity. All tests were made on remotely controlled apparatus in the Solid State Division hot cells.

Three steel containers, each capable of holding eight specimen bars in a helium atmosphere, were fabricated for irradiations in the ORNL graphite reactor. The containers were designated as A, B, and C and were irradiated for successive months. The neutron flux was monitored by using small cobalt foils, and temperatures attained inside the containers were recorded by means of thermocouples. Data on the irradiation of each container are given in Table 8.

A summary of the results of measurements on selected specimens is given in Table 9. Percentage changes and averages for each type of specimen are given in Table 10. Considerable variation will be noted, but this seems to be characteristic of graphite materials. Evidence is sufficient to indicate that much greater damage is to be expected from fission fragments if the particle size of uranium is less than 40 μ. This result is not unexpected, since the average fission-fragment range in graphite is about 15 μ. Larger UO_2 particles would, therefore, trap a larger share of the emitted fission fragments.

The accuracy of measurement is probably as follows: ±0.05% for weight, ±0.3% for electrical resistivity, ±1% for modulus of elasticity, and ±5% for thermal conductivity (average deviations).

Other pertinent data calculated for these experiments are the burnup of uranium in the enriched UO_2 bars, which amounted to 0.1% (0.26 mg), and the fission heat developed per specimen, which was calculated to be about 10 w per specimen (3.1 w/cc). The most unusual result obtained was the large loss of weight in the enriched UO_2 specimens. This loss has not been satisfactorily explained.

In order to measure thermal-conductivity changes, it was necessary to keep one end of each specimen in a molten metal bath at about 160°C and measure the temperature drop at the other end. There has been some indication of an annealing effect as indicated by electrical resistance changes on the control specimens but not on the uranium-bearing specimens after these thermal treatments. Further annealing experiments on all specimens are now being planned, at the conclusion of which a topical report will be published.

RADIATION DAMAGE TO THORIUM AND BERYLLIUM

R. H. Kernohan

Dimensional and hardness measurements were made on six thorium slugs that had been irradiated six months at Hanford. No significant changes were noted in physical dimensions, and there was only a slight increase in hardness. This work was done in cooperation with R. E. Adams of the Metallurgy Division. A more complete program of radiation-damage tests on thorium is being planned.

Dimensional measurements were made on 14 bars of beryllium measuring approximately 0.187 by 0.750 by 2.500 inches. These bars had been irradiated at Hanford for ten months. It was difficult to come to a significant conclusion because preirradiation measurements had not been performed as accurately as postirradiation measurements. However, it would appear that there were no large changes in the bars caused by irradiations. This work was done in cooperation with J. L. Gregg of the Metallurgy Division.

Repeated tests were made on the remotely controlled dimensional-measuring apparatus in order to estimate reliability of results. The average deviation appears to be ±0.0002 in. for the length apparatus and ±0.0005 in. for the thickness and width apparatus.

Table 9

BEFORE AND AFTER IRRADIATION MEASUREMENTS ON GRAPHITE-URANIUM OXIDE BARS

SPECIMEN DESCRIPTION AND NUMBER	CONTAINER	WEIGHT			MODULUS OF ELASTICITY ($\times 10^6$ psi)		ρ, RESISTIVITY AT 20°C (μohm-cm)		ΔT (°C)	
		Before Irrad. (g)	After Irrad. (g)	Difference (mg)	Before Irrad.	After Irrad.	Before Irrad.	After Irrad.	Before Irrad.	After Irrad.
AGOT										
2Z-1	A	4.8897	4.8883	-1.4	0.89	1.28	1127	1566	40.2	49.1
No uranium										
R-1	A	5.6562	5.6555	+1.3	2.96	3.98	1609	1702	61.1	68.2
R-2	B	5.6605	5.6604	-0.1	2.90	4.00	1632	1892	64.5	71.9
R-6	C	5.7851	5.7817	-3.4	2.90	3.96	1644	1874	66.7	72.1
Enriched uranium, 586 μ										
S-5	A	5.5977	5.5700	-27.7	2.90	3.77	1401	1586	68.1	78.1
S-12	B	5.6353	5.6127	-22.6	2.87	3.99	1437	1843	71.8	76.4
S-9	C	5.6499	5.6339	-16.0	2.85	3.95	1421	1733	69.2	72.0
Enriched uranium, 334 μ										
T-6	A	5.6067	5.5750	-31.7	2.85	3.69	1399	1713	62.0	77.4
T-17	B	5.6442	5.6138	-30.4	2.87	3.86	1419	1757	69.5	72.7
T-2	C	5.6399	5.6210	-18.9	2.87	3.84	1430	1675	64.3	70.4
Enriched uranium, 94 μ										
U-7	A	5.5934	5.5210	-72.4	2.92	3.66	1404	1819	66.0	75.5
U-4	B	5.6500	5.5810	-69.0	2.90	3.75	1459	1909	70.6	80.4
U-11	C	5.6101	5.5764	-33.7	2.93	3.91	1430	1774	67.0	74.0
Enriched uranium, <44 μ										
V-3	A	5.5530	5.3566	-196.4	2.82	3.38	1503	2998	67.8	109.9
V-7	B	5.4539	5.2979	-156.0	2.75	3.56	1509	2771	75.8	104.6
V-8	C	5.4560	5.4165	-39.5	2.80	4.34	1510	2502	68.8	101.7
Normal uranium, 586 μ										
X-10	A	5.3684	5.3710	+2.6	2.39	3.08	1612	1893	69.0	76.2
X-4	B	5.4790	5.4775	-1.5	2.70	3.72	1525	1978	76.2	81.3
Normal uranium, 334 μ										
2X-8	B	5.3998	5.3995	-0.3	2.60	3.63	1534	2024	73.4	78.3
2X-4	C	5.4461	5.4384	-7.7	2.55	3.48	1556	1994	72.9	79.7
Normal uranium, 94 μ										
3X-3	B	5.4340	5.4300	-4.0	2.39	3.39	1612	2153	73.0	83.7
3X-6	C	5.4091	5.4034	-5.7	2.47	3.43	1571	2049	69.4	77.8
Normal uranium, <44 μ										
4X-5	A	5.4435	5.4465	+3.0	2.44	3.41	1666	2158	72.7	79.3
4X-4	C	5.4218	5.4123	-9.5	2.45	3.57	1637	2264	75.2	82.6

Table 10

PERCENTAGE OF CHANGES IN PROPERTIES OF IRRADIATED GRAPHITE-URANIUM OXIDE BARS

SPECIMEN DESCRIPTION AND NUMBER	WEIGHT CHANGE (%)	ELASTIC MODULUS INCREASE (%)	ELECTRICAL RESISTIVITY INCREASE (%)	THERMAL CONDUCTIVITY DECREASE (%)
AGOT				
2Z-1	-0.03	44	38.9	22
No uranium				
R-1	+0.02	35	20.8	12
R-2	0.00	38	32.1	12
R-3	-0.06	37	29.8	8
Average	-0.01	37	27.5	11
Enriched uranium, 586 μ				
S-5	-0.50	27	13.2	15
S-12	-0.40	39	28.3	7
S-9	-0.29	39	22.0	4
Average	-0.40	35	21.2	9
Enriched uranium, 334 μ				
T-6	-0.57	30	22.4	25
T-17	-0.54	35	23.8	5
T-2	-0.34	33	17.1	10
Average	-0.48	33	21.1	13
Enriched uranium, 94 μ				
U-7	-1.30	25	29.5	14
U-4	-1.22	29	30.8	14
U-11	-0.60	35	24.0	10
Average	-1.04	30	28.1	13
Enriched uranium, < 44 μ				
V-3	-3.54	20	99.5	62
V-7	-2.86	29	83.6	38
V-8	-0.73	55	65.7	49
Average	-2.38	35	83.0	50
Normal uranium, 586 μ				
X-10	+0.05	29	17.4	10
X-4	-0.03	38	29.7	7
Average	+0.01	34	23.6	9
Normal uranium, 334 μ				
2X-8	-0.01	40	31.9	7
2X-4	-0.14	36	28.1	9
Average	-0.07	38	30.0	8
Normal uranium, 94 μ				
3X-3	-0.07	42	33.6	15
3X-6	-0.11	39	30.4	12
Average	-0.09	41	32.0	14
Normal uranium, <44 μ				
4X-5	+0.06	40	29.5	9
4X-4	-0.18	46	38.3	10
Average	-0.06	43	33.9	10

PART II

CONTENTS

467 029

SUMMARY

SOLID STATE REACTIONS

Position of Bombardment-produced Energy Levels in Germanium. The James-Lehman phenomenological model of defect-produced energy levels was used to obtain values of initial slopes of conductivity vs. bombardment curves as a function of initial hole concentration at −78°C. Energy values were selected to produce a curve giving the best fit with experimental points. The same energy values were used to calculate points for a conductivity vs. bombardment curve and a large discrepancy was found to exist. It was concluded that the saturation hole concentration must increase with bombardment and that the simple model is incapable of explaining experimental observations quantitatively.

Another model that appears to be more nearly in agreement with present experimental data is proposed. This model requires values of a' (ratio of number of states to number of holes in impurity band) greater than 2 for proper agreement on positive slopes. A value of a' greater than 2 is not unreasonable in the light of the James-Lark-Horovitz multilevel model. On the basis of initial slope measurements, it is impossible to test either model sufficiently to determine its validity. Equipment is now available for careful Hall coefficient measurements on bombarded germanium at low temperatures, and it is hoped that the necessary data will be forthcoming.

Germanium Bombardment at −196°C. Conductivity measurements on bombarded germanium have been extended to the temperature of liquid nitrogen in a vertical water-cooled hole in the ORNL graphite reactor. Germanium samples with a wide range of initial carrier concentrations will be studied at this and intermediate temperatures as an aid in locating the defect-produced energy levels in the band scheme of germanium and as a help in deciding on a model.

Radiation Damage in Ionic Crystals. Potassium chloride crystals have been chosen for use in investigating the changes produced in ionic crystals by neutrons and in evaluating the usefulness of ionic-conductivity measurements in solids as a means of studying radiation damage. An ionic-conductivity apparatus and a parallel-balance electrometer tube, a current-measuring device, have been designed and constructed.

Several potassium chloride crystals have been irradiated in hole 51 of the ORNL graphite reactor. Some trouble has been experienced because of the 170-kv betas from the S^{38} produced by a thermal (n,p) reaction. The betas produce ionization in the air of the ionic-conductivity apparatus; this interferes with measurements at the lowest temperatures. A significant enhancement of conductivity has been noted in the low-temperature region.

Radiation Effects on Thermocouples. Thermocouples of copper-constantan, iron-constantan, and copper-iron were exposed in the ORNL graphite reactor, hole D, at reactor ambient temperature for a period of one month. Deviations from normal under these conditions were negligible. Insulation resistance of open thermocouple duplex wires irradiated in the same hole at the same time was of the order of 10^8 ohms.

Determination of the Half Life of Ge^{71} by Electrical Measurements. A high-resistivity, P-type, germanium plate was exposed for 2 hr in the pneumatic tube. Immediately after exposure the sample was heat treated for 40 hr at 450°C to remove the

effects of fast-neutron-induced damage. The conductivity was then recorded as a function of time, with the temperature being maintained at -78°C. The curve obtained corresponds to a calculated half life of 7.55 days for Ge^{71}. Because of the discrepancy between this value and the 11-day half life reported in the literature, an investigation was made of the mobility, which, for the calculations, had been assumed constant during decay. It was found that the mobility increased by 43% during a period of 550 hours. The material was also found to be quite inhomogeneous and to contain multiple P-N junctions.

Equipment is now available with which it should be possible to determine the Ge^{71} half life with a high degree of accuracy when homogeneous samples are available.

Magnetic Susceptibility of Germanium Semiconductors. The balance that will be used in magnetic susceptibility tests has undergone considerable development. Effort is now being concentrated on vibration-free balance mounts and vacuum and cryostatic equipment in the magnet.

Cryostat for Reactor Irradiations. The cryostat has been operated continuously in the ORNL graphite reactor, hole 52, at temperatures of ~100 to 160°C and has been released for experimental work. It is believed that improvements in efficiency can be accomplished to reduce liquid nitrogen consumption and that most of the alterations can be scheduled without disturbing experiments within the sample chamber.

RADIATION METALLURGY

Resolution of Precipitate Nuclei Sizes by Retrogression Phenomena. Copper-beryllium samples were nucleated by irradiation and by aging at 100 and 125°C. Retrogression was noted in hardness and resistance measurements, and a definite resolution was apparent between them. It is concluded that particles responsible for resistance increase are smaller than those which account for hardness increase and that resistance increase caused by nucleation is not related to lattice strain.

Retrogression studies applied to x-ray line shift and broadening resulting from irradiation indicate that the line shift and broadening are associated with nuclei sizes that effect an increase in hardness and are therefore probably caused by coherent lattice strains.

Density Changes in Irradiated Copper-Beryllium Alloy. A density increase of 0.18% has been noted in a copper-beryllium rod exposed to 3.6×10^{18} nvt (fast). This is in agreement with the value calculated from x-ray line-shift measurements for a specimen of similar exposure.

Irradiation-Induced Resistivity Changes in Copper-Beryllium Alloy. A number of in-pile measurements of resistivity were made to verify the existence of a delay time in the resistivity increase. Inconsistency of results is believed to have been caused by variations in heating during attachment of leads. It is estimated that a delay time of about 6 hr would occur in samples unaffected by prior heating.

ENGINEERING PROPERTIES

Physical Properties of Irradiated Elastomers. Compounds containing large amounts of antioxidants and mineral filler were tested to determine the effects of these additives on radiation stability. In no case was the change in radiation stability

great, and in every case in which the percentage of change was less for the compound with the additive, the original strength was less than that of the normal compound.

Since irradiation appears to harden and to increase the specific gravity of many elastomers without evolution of gas, it is suspected that the materials become more crystalline. X-ray diffraction pattern studies will be made to obtain additional data on this subject.

Radiation-Induced Activity in Materials of Construction. Measurements have been completed on the gamma decay of several stainless steels and other alloys and metals that were irradiated in the ORNL graphite reactor. A report containing the decay curves will be issued in the near future.

CRYSTAL PHYSICS

X-Ray Work. A North American Philips x-ray unit was installed. The power supply of this unit may be used to supply the standard Philips tube or may be switched to the Philips high-angle spectrometer or the General Electric hot-cell spectrometer.

The maximum current output available from the G-E tube using the Philips power source is 7 ma, which is not as great as desired but which, nevertheless, permits the spectrometer to be utilized for some types of experiments. The spectrometer is still in its bench-test position outside the hot cells and is being used to obtain rocking-curve data from copper single crystals.

A study has been initiated to determine whether radiation produces changes in the crystal structures of plastics and elastomers.

SPECIAL PROJECTS

Radiation Damage to Miscellaneous Materials. Resistivity measurements were made on copper-gold samples of both ordered and disordered lattice structure. Irradiation produced little change in the disordered specimen but caused the resistivity of the ordered specimen to increase by a factor of approximately 2.

SOLID STATE REACTIONS

POSITION OF BOMBARDMENT-PRODUCED ENERGY LEVELS IN GERMANIUM

J. H. Crawford, Jr. J. W. Cleland

The observed behavior of the electrical conductivity of P-type germanium under fast-neutron bombardment can be qualitatively explained by the phenomenological model of defect-produced energy levels proposed by James and Lehman.[1] The results of this model were expressed in a previous report[2] in a convenient form for quantitative comparison with experiment. Under the assumptions that

(1) J. W. Cleland, J. H. Crawford, Jr., H. Lark-Horovitz, J. C. Pigg, and F. W. Young, Jr., *Phys. Rev.* 84, 861 (1951).

(2) J. H. Crawford and J. W. Cleland, *Solid State Division Quarterly Progress Report for Period Ending January 31, 1952*, ORNL-1261, p. 5.

(1) Frenkel defects alone are introduced, (2) all chemical acceptors are completely ionized, and (3) both defect-produced acceptors and hole traps are completely ionized, the model predicts that the initial slope of the hole concentration vs. defect concentration curve for P-type germanium obeys the relation

$$\left(\frac{dn_h}{dN}\right)_I = S_I$$

$$= \frac{K_1 - (n_h^0)^2 K_2}{(n_h^0)^2 K_2 + n_h^0 (K_1 K_2 + 1) + K_1} , \quad (1)$$

where K_1 and K_2 are the equilibrium constants for acceptor ionization and hole trapping, respectively, and n_h^0 is the initial hole concentration due to chemical acceptors. In addition, the saturation or limiting hole concentration at which the slope is zero is given by

$$n_h^* = \left(\frac{K_1}{K_2}\right)^{1/2} . \quad (2)$$

The equilibrium constants are

$$K_1 = \left[\frac{2(2\pi m_h kT)^{3/2}}{h^3}\right] e^{-\Delta\epsilon_1/kT}$$

and (3)

$$K_2 = \frac{h^3 \; e^{\Delta\epsilon_2/kT}}{2(2\pi m_h kT)^{3/2}} ,$$

where $\Delta\epsilon_1$ is the ionization energy of the defect acceptor, $\Delta\epsilon_2$ is the depth of the hole trap, and m_h is the effective mass of a hole (presumed to be equal to the rest mass of an electron in all calculations). Thus

$$n_h^* = \left[\frac{2(2\pi m_h kT)^{3/2}}{h^3}\right] e^{-(\Delta\epsilon_1 + \Delta\epsilon_2)/2kT}$$

$$= (4.82 \times 10^{15} T^{3/2}) \, e^{-\zeta^*/kT} , \quad (4)$$

where ζ^* is the limiting value of the Fermi level.

At -78°C the limiting hole concentration as determined from the initial slopes of conductivity vs. bombardment curves is $(1.5 \pm 0.2) \times 10^{15}$, which corresponds to a ζ^* of 0.154 ± 0.003 ev. The value of $(dn_h/dN)_I$ is obtained from the initial slope of the conductivity vs. bombardment curve by the relation

$$\left(\frac{dn_h}{dN}\right)_I = \frac{1}{Ce\mu_h} \left[\frac{d\sigma}{d(nvt)_{fast}}\right]_I , \quad (5)$$

where e is the electronic charge, μ_h is the hole mobility, and C is the number of acceptors or traps introduced per incident neutron. The value of C is unknown and cannot be determined directly. However, it is assumed that it is identical with the rate of removal of electrons from low-resistivity N-type germanium at room temperature. According to a model proposed by James and Lark-Horovitz,[3] which assigns multiple energy levels to interstitials and vacancies, this assumption is somewhat in question, and the value of C so chosen may be high by a factor of 2. However, the results of this analysis are not invalidated by the choice of the value of C, since a number of values were used in the analysis with not much better agreement.

[3] H. M. James and K. Lark-Horovitz, *Z. physik. Chem.* **198**, 107 (1951).

467 033

ACTUAL MS PG ______ GALLEY NO. ______

DECLASSIFIED

TYPIST ______ SAME SIZE TIS Form 131 (Rev. Sep. 1953)

Figure 14 shows a plot of the initial slope vs. initial hole concentration at -78°C. The points were determined from experimental data. The curve that fits the data best was determined from Eq. 1 by using $\Delta\epsilon_1 = 0.215$ ev and $\Delta\epsilon_2 = 0.093$ ev. These energy values were used in an attempt to fit a number of bombardment curves for samples whose initial hole concentrations were less than the observed saturation value. Figure 15 shows the results of this attempt for a typical curve. The calculated points are shown by dots, and it is obvious that a large discrepancy exists if these energy values are used. The second set of points, indicated as circles, were calculated by using $\Delta\epsilon_1 = 0.160$ ev, $\Delta\epsilon_2 = 0.083$ ev, and $C = 0.59$. An excellent fit is obtained, but these energy values correspond to $n_A^\circ = 1 \times 10^{16}$ cm^{-3}, which is higher than the observed value by a factor of 7, and the value of C is only one-fourth the expected value.

The model as used here assumes that the concentration of acceptors is equal to the concentration of hole traps. An attempt was made to improve the fit by using a ratio of hole-trap concentration to acceptor concentration, a, greater than unity. Except for unreasonably large values of a, the energy values required to fit the bombardment curve were incompatible

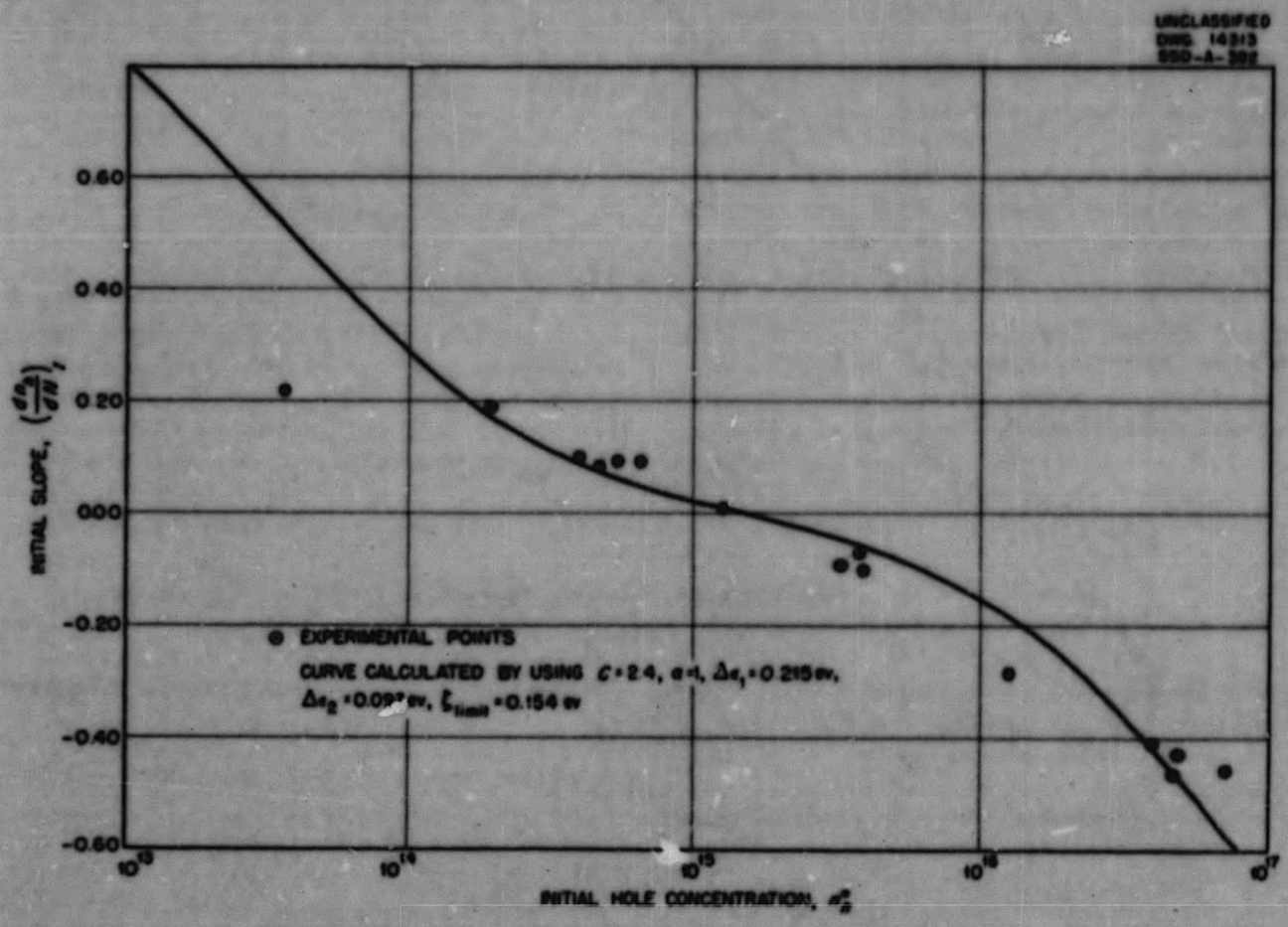

Fig. 14. Initial Hole Concentration vs. Initial Slope for P-Type Germanium at -78°C.

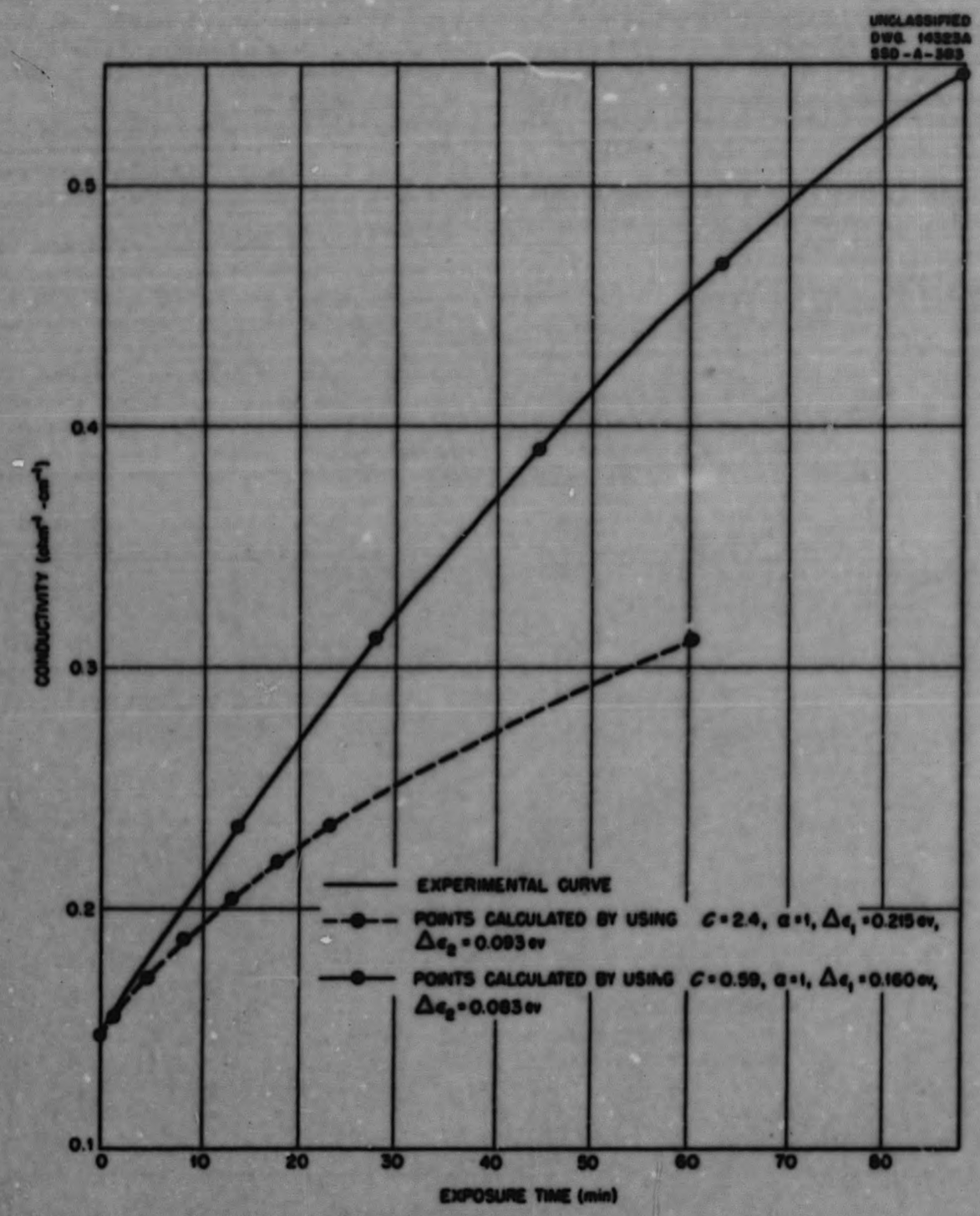

Fig. 15. Conductivity vs. Bombardment for P-Type Germanium ($n_h^0 = 1.90 \times 10^{14}$ cm^{-3}) at -78°C.

with the saturation hole concentration values obtained from initial slope data. The results of these analyses seem to indicate that the saturation hole concentration increases with bombardment. In this connection Forster[4] has observed a conductivity minimum in deuteron bombardment curves on material with $10^{15} < n_A^0 < 5 \times 10^{17}$ at -72°C. Minimums occur at integrated fluxes of the order of $10^{17}/cm^2$, which are values greater than have been obtainable with the present equipment in the ORNL graphite reactor. In addition, Forster finds that n_A^0 at -72°C is 3.5×10^{16} cm^{-3}, which is a value higher than that reported here by a factor of 20 and much too large to be explained by the difference in temperature.

The simple model is inadequate in the following respects: (1) the lack of agreement between energy values determined from initial slope data and those obtained from bombardment curve fitting, (2) the apparent discrepancy between n_A^0 determined from initial slopes and curve fitting, and (3) the minimum in the conductivity vs. bombardment curve observed by Forster upon using deuterons on P-type germanium. Thus it is evident that the simple model as used here is incapable of explaining experimental observation quantitatively.

There are two factors that have not been considered in the simple model: a distribution in energy of the defect-produced states and the possibility of annealing out the defects. The latter may be a differential annealing in which one type of state (acceptor or hole trap) may anneal out more rapidly than the other. This could be caused by a clustering of either vacancies or interstitials. This latter effect would explain the apparent change in n_A^0 with bombardment. On the other hand, if an energy distribution is present, it is possible that conduction could take place to some extent in such a band of levels and that this becomes sufficiently important for high defect concentration to produce a minimum in the conductivity vs. bombardment curve. Such an effect has been observed by Hung and co-workers[5] in the case of chemical impurities at very low temperatures.

The effect of a distribution of energy levels may be examined by using the following model. Instead of discrete levels of acceptors and hole traps, a uniform distribution of levels may be considered that contains $\alpha' N_A$ states and adds only N_A holes to the total to be considered (where α' is greater than 1). Thus,

$$\int_{\epsilon_1}^{\epsilon_2} n_A(\epsilon)\, d\epsilon = n_A^0 + N_A \,. \qquad (6)$$

The position and density of the level distribution is

$$g(\epsilon) = A, \quad \text{for } \epsilon_1 \leq \epsilon \leq \epsilon_2$$

and (7)

$$g(\epsilon) = 0, \quad \text{for } \epsilon < \epsilon_1, \quad \epsilon > \epsilon_2 \,,$$

where $g(\epsilon)$ is the density of the states per unit energy interval, ϵ_1 and ϵ_2 are the lower and upper limits of the distribution, respectively, and are measured from the top of the filled band, and A is a constant for a given period of irradiation. If annealing is appreciable, A will be both temperature and time dependent. Thus,

$$A = \frac{\alpha' N_A}{\epsilon_2 - \epsilon_1} \,. \qquad (8)$$

[4] J. Forster, private communication.

[5] C. S. Hung and J. R. Gliessman, *Phys. Rev.* 79, 726 (1950); C. S. Hung, *op. cit.*, p. 727.

The integral of Eq. 1 may be separated into two parts: one from 0 to ∞, and the other from 0 to $-\infty$. When Fermi-Dirac statistics are used,

$$\int_{-\infty}^{0} n(\epsilon)\,d\epsilon = \left[\frac{2(2\pi mkT)^{3/2}}{h^3}\right] e^{-\zeta/kT} \quad (9)$$

and

$$\int_{0}^{\infty} n(\epsilon)\,d\epsilon = \int_{\epsilon_1}^{\epsilon_2} \frac{g_h(\epsilon)\,d\epsilon}{e^{(\zeta-\epsilon)/kT}+1}$$

$$= AkT\left[\frac{\epsilon_2-\epsilon_1}{kT} + \ln\frac{e^{(\zeta-\epsilon_2)/kT}}{e^{(\zeta-\epsilon_1)/kT}+1}\right]. \quad (10)$$

Combining Eqs. 9 and 10 and using the value of A from Eq. 8, gives for Eq. 6,

$$n_h^0 + N_h = \left[\frac{2(2\pi mkT)^{3/2}}{h^3}\right] e^{-\zeta/kT}$$

$$+ \alpha' N_h + \frac{\alpha' N_h kT}{\epsilon_2-\epsilon_1} \ln\left[\frac{e^{(\zeta-\epsilon_2)/kT}+1}{e^{(\zeta-\epsilon_1)/kT}+1}\right]. \quad (11)$$

Equation 12 may now be expressed in terms of hole concentration by means of the relation,

$$n_h = \left[\frac{2(2\pi mkT)^{3/2}}{h^3}\right] e^{-\zeta/kT}$$

$$= C(T)\, e^{-\zeta/kT}. \quad (12)$$

Thus,

$$n_h = n_h^0 - N_h(\alpha' - 1)$$

$$+ \frac{\alpha' NkT}{\epsilon_2-\epsilon_1} \ln\left[\frac{C(T)\, e^{-\epsilon_1/kT} + n_h}{C(T)\, e^{-\epsilon_2/kT} + n_h}\right]. \quad (13)$$

The limiting hole concentration and the initial variation of n_h and N_h are readily obtained from Eq. 13.

$$n_h = \frac{C(T)\left(e^{-\epsilon_1/\alpha' kT} - e^{-\epsilon_2/\alpha' kT}\right)}{e^{(\alpha'-1/\alpha')(\epsilon_2/kT)} - e^{(\alpha'-1/\alpha')(\epsilon_1/kT)}} \quad (14)$$

and

$$\left(\frac{dn_h}{dN_h}\right)_I$$

$$= 1 - \alpha' + \frac{\alpha' kT}{\epsilon_2-\epsilon_1} \ln\left[\frac{C(T)\, e^{-\epsilon_1/kT} + n_h^0}{C(T)\, e^{-\epsilon_2/kT} + n_h^0}\right] \quad (15)$$

If the defect band is half filled, $\alpha' = 2$, Eq. 15 reduces to

$$n_h^* = C(T)\, e^{-(\epsilon_2-\epsilon_1)/2kT}, \quad (16)$$

and ζ^* lies in the middle of the defect band.

Calculations of $(dn_h/dN_h)_I$ as a function of n_h^0 for three different band widths ($\Delta\epsilon = 0.07$ ev; $\Delta\epsilon = 0.10$ ev; $\Delta\epsilon = 0.15$ ev) and for $\alpha' = 2$ are shown in Fig. 16. The experimental points, calculated when $C = 1.2$, are shown as X's. For negative slopes, experimental and calculated values seem to compare rather favorably. For positive slopes, however, observed values appear to be about a factor of 2 lower than the calculated values. This would seem to indicate that a larger value of α' is necessary to give a fit to the experimental data. In the light of the James-Lark-Horovitz multilevel model,[3] a value of α' greater than 2 (the defect band less than half filled) is not unreasonable.

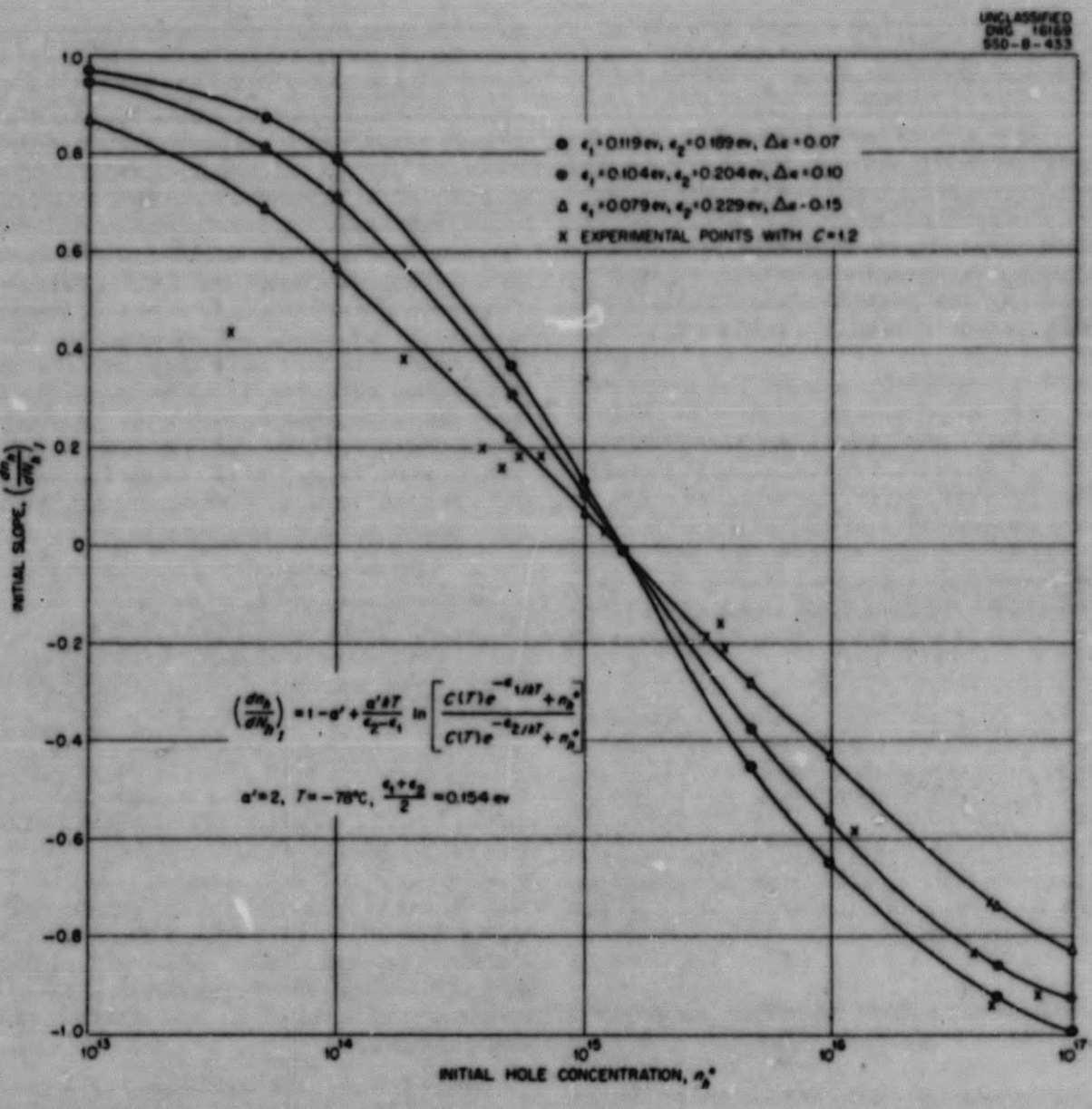

Fig. 16. Initial Hole Concentration vs. Initial Slope for Three Band Widths of P-Type Germanium.

On the basis of initial slope measurements it is impossible to test either model sufficiently to determine its validity. Not only must the model fit extensive bombardment curves, but in addition it must be capable of predicting the temperature-dependence of hole concentration. Equipment is now available for careful Hall coefficient measurements on bombarded germanium at low temperatures and for longer low-temperature bombardment periods. It is hoped that the necessary data will be available in the near future.

GERMANIUM BOMBARDMENT AT -196°C

J. W. Cleland J. H. Crawford, Jr.
J. C. Pigg

Conductivity measurements on germanium have been extended to the temperature of liquid nitrogen (-196°C) by the use of quartz Dewar vessels. With these it is possible to maintain liquid nitrogen for periods up to 3 hr in a vertical water-cooled hole in the ORNL graphite reactor (hole 12).

Two P-type germanium samples were exposed at the temperature of liquid nitrogen, and their conductivities were followed during the exposure. The initial rates of hole removal at this temperature were 0.57 per incident neutron for the sample whose initial hole concentration was 1.2×10^{15} cm^{-3} and 0.79 per incident neutron for the sample whose initial hole concentration was 1.9×10^{15} cm^{-3}.

It is planned to study germanium samples with a wide range of initial carrier concentrations at this and intermediate temperatures. Such experimental data will aid greatly in location of defect-produced energy levels in the band scheme of germanium and will help in deciding on a model for these levels.

RADIATION DAMAGE IN IONIC CRYSTALS

R. L. Sproull

A study of reactor irradiation of potassium chloride crystals has been undertaken. The two main purposes of this study are to explore the phenomena of changes in ionic crystals produced by neutrons and to evaluate the usefulness of ionic-conductivity measurements as a tool to study displacements produced by neutrons in solids. Since ionic conductivity at temperatures less than 500°C in potassium chloride is proportional to the number of potassium-ion vacancies, information is expected about the creation of such vacancies by fast neutrons.

Potassium chloride was chosen for this study primarily because systematic studies of ionic conductivity as a function of added divalent cations have been made on this salt. Another feature of potassium chloride that may be an advantage in the interpretation of experiments is the near-equality of mass of the anion and cation. The nuclear properties of potassium chloride are not unsuitable for the experiments planned, although some other alkali halides would be preferable (e.g., potassium fluoride, but few solid-state experiments have been made on this compound).

An ionic-conductivity apparatus and a current-measuring device with a parallel-balance electrometer tube have been designed and constructed. The ionic conductivity of Harshaw potassium chloride crystals has been studied before irradiation. The data obtained agree with what appears to be the best published material,[6] and appreciably extend the temperature range of ionic-conductivity information. These experiments show that the Harshaw crystals are adequately pure for the neutron irradiation studies contemplated. The suitability of both sputtered-platinum and painted-graphite electrodes has also been established.

Several crystals have been irradiated in hole 51 of the ORNL graphite reactor for an estimated 1.2×10^{18} nvt (fast). The only troublesome activity comes from a thermal (n,p) reaction that produces 87-day S^{35}. The 170-kv betas from these nuclei produce ionization in the air of the ionic-conductivity apparatus; such ionization gives a background that interfers with ionic-conductivity measurements at the lowest

(6) H. Kelting and R. Witt, *Z. Physik* 120, 697 (1949).

temperatures. A helium atmosphere is being used to minimize this effect, but redesign to permit evacuation of the apparatus would be desirable.

As was expected, irradiation of this order of magnitude produced no change in ionic conductivity in the intrinsic (high-temperature) region. A significant enhancement of conductivity seems to have occurred in the structure-sensitive (low-temperature) region. Experiments are in progress to study the kinetics of the annealing-out of this enhancement, to find the dependence on nvt (fast), and to make sure that this is a neutron effect (rather than an effect produced by large gamma exposure).

RADIATION EFFECTS ON THERMOCOUPLES

J. C. Pigg

Tests have been made to detect and study changes in thermocouple output emf owing to reactor irradiation. The thermocouples were made from copper-constantan and iron-constantan duplex thermocouple wires with the two junctions soldered together. The copper-constantan, iron-constantan, and copper-iron potentials were recorded. These voltages were converted to temperature, and the temperatures measured by the three thermocouples were compared. For an exposure period of 31 days in hole D in the ORNL graphite reactor no deviation was observed in the relative output of the various couples greater than 0.1°C (approximately the limit of accuracy of the measurement). Thus it can be concluded that, at reactor ambient temperature, effects of fast-neutron-induced radiation damage in thermocouples composed of these materials are negligible for general use for a period of one month.

The insulation resistance of open thermocouple duplex wires irradiated at the same time in the same hole was of the order of 10^8 ohms.

DETERMINATION OF THE HALF LIFE OF GERMANIUM-71 BY ELECTRICAL MEASUREMENTS

J. W. Cleland J. H. Crawford, Jr.
J. C. Pigg

The effect of nuclear transformations resulting from thermal-neutron activation of the various germanium isotopes on the electrical properties of bulk germanium has been extensively studied.[7] The various nuclear reactions involved are listed in Table 11, together with their thermal-activation cross sections. Since gallium is an acceptor impurity and arsenic is a donor impurity, the net result after decay is an increase in the P-type character of bulk germanium. However, because of the large difference between the half lives of the gallium-producing activity and the arsenic-producing activities, the material should become more N-type initially. Except for the effect of the decaying As^{77}, which is relatively small (10% of the total introduced arsenic concentration), the neutron-produced

(7) J. W. Cleland, K. Lark-Horovitz, and J. C. Pigg, *Phys. Rev.* 78, 814 (1950).

Table 11

NUCLEAR REACTIONS OF GERMANIUM ISOTOPES

REACTION	ATOMIC CROSS SECTION* (barns)
$Ge^{71} \xrightarrow{11\ d} Ga^{71}$	0.69
$Ge^{75} \xrightarrow{82\ m} As^{75}$	0.22
$Ge^{77} \xrightarrow{59\ s} As^{77} \xrightarrow{40\ h} Se^{77}$ $Ge^{77} \xrightarrow{12\ h} As^{77} \xrightarrow{40\ h} Se^{77}$	0.02

*H. Pomerance, *Physics Division Quarterly Progress Report for Period Ending December 15, 1949*, ORNL-577, p. 25.

arsenic concentration is essentially constant after the first few hours. If the conductivity as a function of time after irradiation is followed, the rate of production of Ga^{71} can be observed directly.

A high-resistivity P-type germanium plate was exposed for 2 hr in the pneumatic tube. Immediately after exposure, the sample was heat treated for 40 hr at 450°C to remove the effects of fast-neutron-induced damage. The conductivity of the plate was then recorded as a function of time, the temperature being maintained constant at -78°C. A plot of the conductance vs. time at this temperature is shown in Fig. 17.

The half life can be readily calculated from the conductance vs. time curve if the effect of the decay of Ge^{77} is neglected. If it is assumed that the mobility remains constant during radioactive decay, the change in conductance for a given time interval is proportional to the change in the Ga^{71} concentration. The latter is given by

$$\Delta N_{Ga^{71}} = N^0_{Ge^{71}} (1 - e^{-k't}) , \quad (1)$$

where $N^0_{Ge^{71}}$ is the concentration of Ge^{71} at the beginning of the measurement at which t is arbitrarily taken as zero, and k' is the rate constant. The half life is obtained from the relation

$$t_{1/2} = \frac{1}{k'} \ln 2 . \quad (2)$$

For location of the calculated points of Fig. 17, $k' = 3.85 \times 10^{-3}$, which corresponds to a half life of 7.55 days, was used. The value reported for the Ge^{71} half life is 11 days.[8] Because of this discrepancy, the Hall coefficient measurements that were taken periodically during the decay period were used to check the assumption of constant mobility. It was found that the mobility increased considerably during the period of observation (43% during 550 hr). Further examination of the sample showed that the material was quite inhomogeneous and that it contained multiple P-N junctions. The combined effect of varying mobility and potential barriers associated with the P-N junctions introduces considerable uncertainty into the half-life determination.

This experiment will be repeated when material of better homogeneity is available. The relative precision of measurement is sufficiently great (approximately 0.05%), with the equipment employed, that with homogeneous samples it should be possible to determine the Ge^{71} half life with a high degree of accuracy.

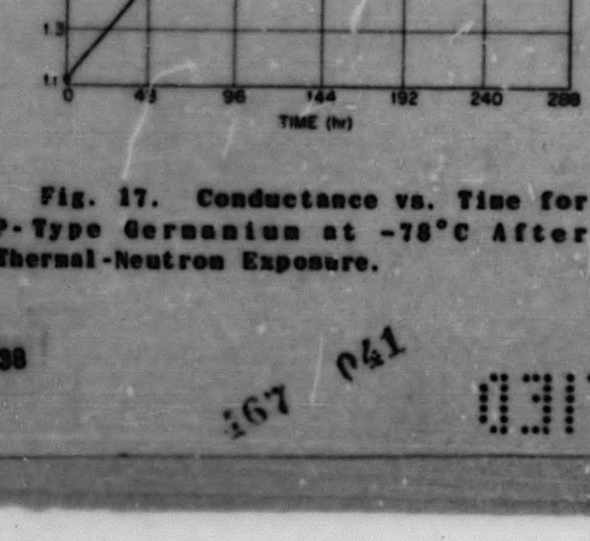

Fig. 17. Conductance vs. Time for P-Type Germanium at -78°C After Thermal-Neutron Exposure.

(8) *National Bureau of Standards Nuclear Data*, NBS-499 (Sept. 1, 1950).

MAGNETIC SUSCEPTIBILITY OF GERMANIUM SEMICONDUCTORS

D. K. Stevens

The balance, previously described,[9] that will be used in magnetic susceptibility tests has undergone considerable development. Elgiloy has been substituted for beryllium-copper alloy as the main suspension, and supports with adjustable net coefficients of thermal expansion have been added for the speaker magnet and microformer. Considerable effort has been expended in improving the circuitry associated with the microformer detector. At the present time, a circuit that was designed by R. L. Sproull and which employs a parallel-balanced amplifier followed by a phase-sensitive detector appears to make force measurements in the microgram region feasible.

Present efforts are being directed toward the design and construction of balance mounts and vacuum and cryostatic equipment in the magnet. A major problem will be the isolation of the balance from sources of mechanical vibration.

CRYOSTAT FOR REACTOR IRRADIATIONS

R. P. Metcalf[10] J. T. Howe

The vacuum difficulties encountered in the cryostat, which is located in hole 52 of the ORNL graphite reactor, were cleared up during this quarter. The cryostat was test-operated for one week at temperatures of -100 to -160°C that were controlled from a thermocouple located on a dummy specimen within the sample chamber.

Liquid nitrogen consumption was considered excessive in comparison with consumption in preinstallation bench tests. Bench-test consumption was 1.8 liters/hr at -100°C, 2.2 liters/hr at -130°C, and 2.6 liters/hr at -150°C; in-pile consumption was 5 liters/hr at -100°C and 7 liters/hr at -150°C. Some of the heat loss may be attributed to the fact that two elbows on the vacuum jacket of the helium line to the cryostat build up considerable frost during operation, which indicates that the inside lines are probably touching the jacket. Another reason for higher consumption is that the reactor ambient temperature is considerably higher than room temperature; the temperature within the sample chamber was measured at +145°C with all cooling facilities shut off. The design provides for a cooling jacket to surround the cryostat, however, so that the effective reactor temperature may be reduced by air or water flow. A temperature rise of about 10°C in the air flow through this cooling jacket has not been sufficient to produce a measurable decrease in nitrogen consumption. Outlet-water cooling from hole 51 will be substituted for the air in an effort to lower the nitrogen consumption in the future.

(9) D. K. Stevens, *op. cit.*, ORNL-1261, p. 7.

(10) Metcalf is at present with the Materials Chemistry Division, but he has made available design and operating knowledge gained in past work with the cryostat.

RADIATION METALLURGY

RESOLUTION OF PRECIPITATE NUCLEI SIZES BY RETROGRESSION PHENOMENA

G. T. Murray W. E. Taylor

It has been shown in a previous report[1] that if precipitate particles of different sizes are responsible for observed changes in different properties (i.e., resistance and hardness), then this fact can be determined by means of retrogression studies. A number of hardness and resistance samples of copper-beryllium alloy were nucleated by irradiation and by aging at 100 and 125°C to produce approximately 10% increase in resistivity. The samples were then held at temperatures between 125 and 375°C for brief periods of time, and the amount of retrogression was determined. The retrogression, measured as $\Delta P'/\Delta P$, where $\Delta P'$ is the amount of recovery and ΔP is the original change of the property P owing to nucleation, is shown in Fig. 18 as a function of temperature. There is considerable variation of the data even within one set of samples, but the data for all tests fall within well-defined scatter bands that clearly show a resolution between the retrogression of resistance and hardness. The fact that the resistance retrogression occurs at a lower temperature than that for hardness indicates that the particles responsible for resistance increase are smaller than those which account for the hardness increase. At 300°C there is almost no retrogression of hardness, which indicates that most of the lattice strain is still present. Since at this temperature the retrogression of resistance is nearly complete, it appears that the resistance increase caused by nucleation is not related to lattice strain.

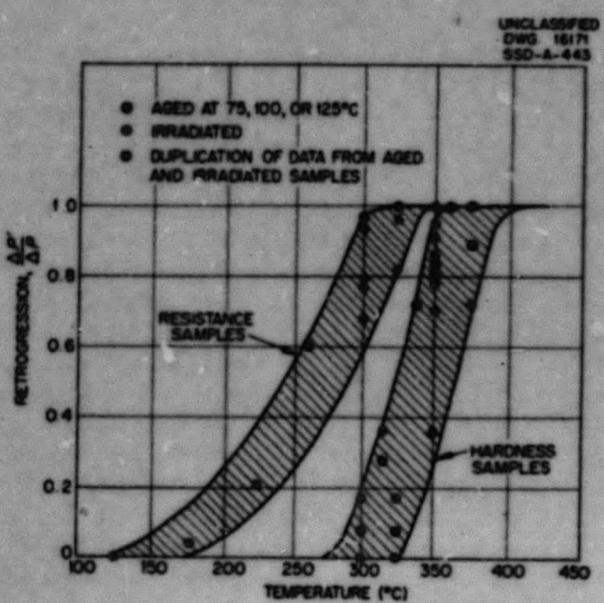

Fig. 18. Regrogression in Copper-Beryllium Alloys as a Function of Temperature, Measured by Resistance and Hardness.

The possibility that the recovery is related to growth of the nuclei is discounted by the rapidity of the retrogression as compared to property changes known to be associated with precipitate growth (Fig. 19).

The x-ray line shift and broadening that result from irradiation have also been subjected to retrogression investigations. Solution-annealed filings were irradiated and then aged with nonirradiated comparison standards at 300 and 350°C. At the lower temperature no change in the line shape or position was observed in either the irradiated or standard specimens after 30 sec of annealing. At 350°C no change was observed in the standard specimen after 30 sec, but about 75% recovery was observed for the irradiated filings. The results are shown in

(1) W. E. Taylor and G. T. Murray, *Solid State Division Quarterly Progress Report for Period Ending January 31, 1952*, ORNL-1261, p. 10.

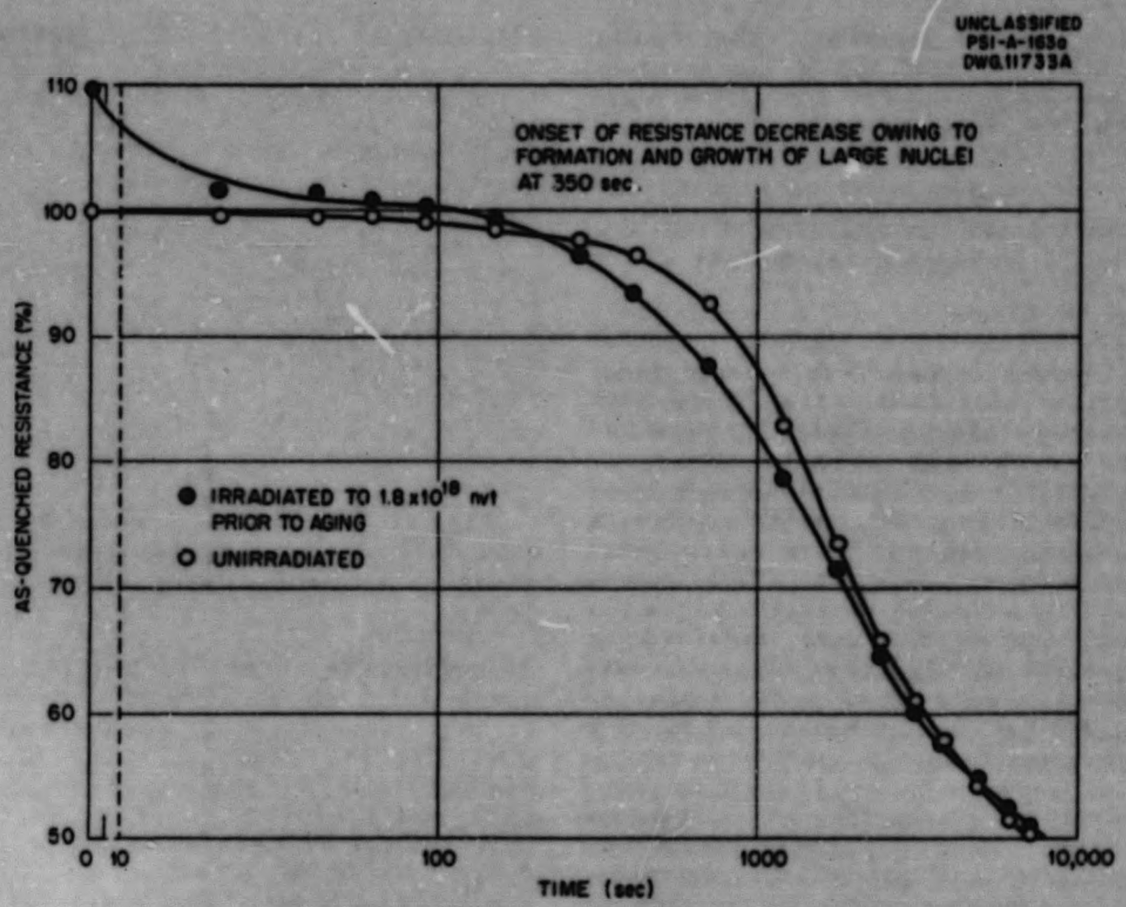

Fig. 19. Effect of Neutron Irradiation on Subsequent Aging of Copper-Beryllium Alloy at 323°C.

Fig. 20. These data indicate that the x-ray line shift and broadening are associated with nuclei sizes that effect an increase in hardness and are therefore probably caused by coherent lattice strains.

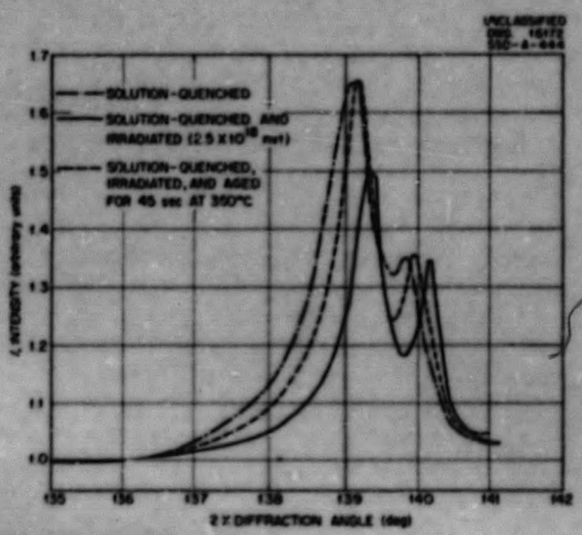

Fig. 20. Retrogression Effect on (331) Line in Irradiated Cu-Be Alloy at 350°C.

DENSITY CHANGES IN IRRADIATED COPPER-BERYLLIUM ALLOY

G. T. Murray W. E. Taylor

Density measurements were made by the immersion method on two copper-beryllium rods approximately 1/4 in. in diameter and 2 in. long. One specimen was exposed to 3.8×10^{18} nvt (fast) and the other specimen was retained as a standard. An increase in density of 0.18% was observed for

the irradiated specimen. This result is in good agreement with the increase in density of 0.19% for 3.9×10^{18} nvt calculated from the x-ray line shift.

RADIATION-INDUCED RESISTIVITY CHANGES IN COPPER-BERYLLIUM ALLOY

W. E. Taylor F. M. Blacksher

A number of short in-pile measurements of resistivity has been made to verify the existence of a delay time in the resistivity increase. Resistivity determinations were made by applying the voltage drop across a standard resistance and that across the specimen to a Brown multipoint recording potentiometer having a scale from 20 to 25 mv. The temperature of the specimen was simultaneously determined by recording the output of an iron-constantan thermocouple on a Brown recorder.

The results shown in Fig. 21 are not consistent with respect to delay time or initial slope. The variations are believed to be due to heating of the sample while leads were being soldered. Tests are now being made to determine the effect of heating the sample for 5 min at 75°C on the amount of resistance increase during a one-week irradiation. All the tests showed a delay time between the initiation of irradiation and the onset of the resistance change. The delay time varied between 1 and 3 hr, and it is estimated that a delay time of about 6 hr would occur in samples unaffected by prior heat.

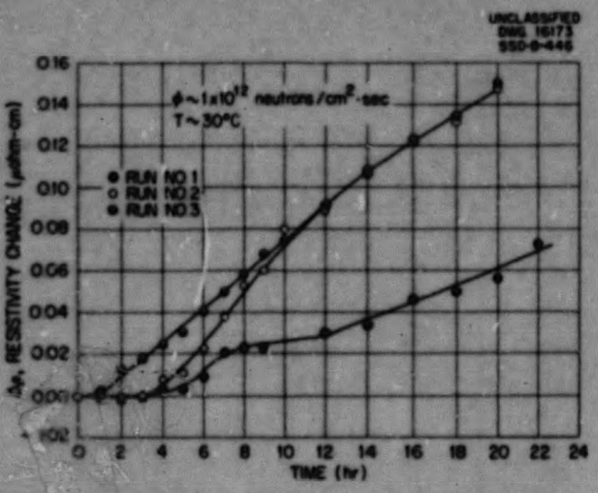

Fig. 21. Resistivity Change During Early Stages of Irradiation-Aging of Solution-quenched Copper-Beryllium Alloy.

ENGINEERING PROPERTIES

PHYSICAL PROPERTIES OF IRRADIATED ELASTOMERS

C. D. Bopp R. L. Towns
O. Sisman W. K. Kirkland

Compounds containing large amounts of antioxidants and mineral filler were tested[1] to determine the effect of these additives on radiation stability. The recipes used are listed in Table 12 along with the normal compound. The results for two irradiation periods are shown in Table 13. The antioxidants and the mineral fillerwere added in an attempt to improve the stability of the elastomers. In both cases the change in radiation stability was not great, but the percentage of change in some properties is less for the recipes with the additives than for the normal recipe. In every case, however, where the percentage of change was less for the compound with the additive, the original strength was also much less than for the normal compound, with the net result that no

[1] O. Sisman, C. D. Bopp, W. K. Kirkland, and R. L. Towns, *Physics of Solids Institute Quarterly Progress Report for Period Ending July 31, 1951*, ORNL-1128, p. 41.

Table 12

COMPOSITIONS OF ELASTOMERS

COMPONENTS	ELASTOMERS (parts by weight)					
	Neoprene W	Neoprene W with Dodecyl Mercaptan	Natural Rubber	Natural Rubber with Dodecyl Mercaptan	Natural Rubber with Dibutyl Tin Dilaurate	Natural Rubber with Asbestos Filler
Neoprene W	100.0	100.0				
Natural rubber			100.0	100.0	100.0	100.0
Zinc oxide	5.0	5.0	5.0	5.0	5.0	5.0
Phenyl beta naphthylamine	1.0	2.0	1.0		1.0	1.0
SRF black	45.0	40.0	70.0	70.0	70.0	
Stearic acid	0.5	0.5	1.0	1.0	1.0	1.0
Magnesium oxide	2.0	2.0				
Permalux	0.5					
Accelerator		0.5				
Dodecyl mercaptan		10.0		10.0		
Captax			0.6		0.6	0.6
Sulfur			3.0		3.0	3.0
Lead oxide				10.0		
Chloranil				5.0		
Dibutyl tin dilaurate					10.0	
Asbestos filler						250.0
Total parts	154.0	160.0	180.6	201.0	190.6	360.6

improvement was effected for the irradiation periods shown. A definite improvement in resistivity was found for all the special recipes, especially that with the mineral filler additive.

Natural rubber is hardened by irradiation, whereas butyl rubber is softened. It was thought that perhaps by compounding the two in the right proportions a material would result that was more radiation-resistant than either of the original materials. Four such mixtures (Table 14) were tried. Results for two irradiation periods are shown in Table 15. None of the mixtures showed any real improvement over natural rubber, which is the more radiation-resistant of the two. The change in durometer hardness is less for both the 50:50 and 25:75 mixtures than for natural rubber; however, the decrease in tensile strength and elongation is more pronounced for the mixture than for natural rubber.

A sample of Vulcollan was recently obtained from the B. F. Goodrich Company. This elastomer is not yet produced commercially, since it is still in the developmental stage. It has the following structure:

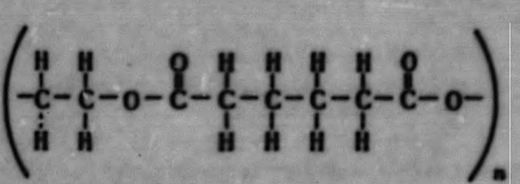

Table 13

RADIATION-PRODUCED CHANGES IN PHYSICAL PROPERTIES OF SPECIALLY COMPOUNDED ELASTOMERS

	ELASTOMERS					
	Neoprene W	Neoprene W with Dodecyl Mercaptan	Natural Rubber	Natural Rubber with Dodecyl Mercaptan	Natural Rubber with Dibutyl Tin Dilaurate	Natural Rubber with Asbestos Filler
Irradiation exposure (10^{18} nvt)	0	0	0	0	0	0
	0.25	0.25	0.25	0.25	0.25	0.25
	0.60	0.60	0.60	0.60	0.60	0.60
Tensile strength (psi)	2900	1500	2600	2100	2900	1100
	1200	800	2000	1400	1300	1000
	900	800	1300	350	750	1200
Elongation (%)	450	440	420	280	220	90
	50	40	250	100	110	40
	20	10	110	10	40	10
Shore durometer hardness	78	79	61	65	68	83
	90	84	72	75	76	94
	98	92	80	86	82	97
Shore elasticity	85	72	100	83	75	30
	45	40	70	60	40	25
	-	25	50	20	30	-
Compression set (%)						
Strain immediately after application of load	31	26	30	25	22	15
	8		18			
	3	3	14	12	6	4
Final deformation	9	60	13.0	6	11	10
	2		7.1			
	2	3.4	4.5	1.6	3	1.1
Specific gravity (25°/4°C)	1.418	1.356	1.186	1.22	1.19	1.72
	1.423	1.363	1.187	1.22	1.19	1.72
	1.444	1.379	1.192	1.23	1.19	1.73
Change in weight (%)	-	-	-	-	-	-
	-	-	-	-	-	-
	0.10	0.28	-0.03	0.03	-0.16	0.02
Volume resistivity (ohm-cm)	10^{11}	10^{11}	10^{10}	10^{11}	10^{12}	10^{11}
	10^{8}	-	10^{10}	-	-	-
	10^{8}	10^{12}	10^{11}	10^{11}	10^{12}	$> 10^{12}$
Dielectric strength (v/mil)	300	300	200	120	115	> 400
	300	360	200	120	115	400
	200	380	150	-	115	400

Table 14

COMPOSITIONS OF NATURAL AND BUTYL RUBBER COMBINATIONS

COMPONENTS	ELASTOMERS (parts by weight)			
	Natural Rubber to Butyl, 50:50	Natural Rubber to Butyl, 25:75	Natural Rubber to Butyl, 10:90	Natural Rubber to Butyl Reclaim, 100:60
Natural rubber	50.0	25.0	10.0	100.0
Butyl rubber	50.0	75.0	90.0	
Zinc oxide	5.0	5.0	5.0	5.0
SRF black	70.0	70.0	70.0	70.0
Stearic acid	2.0	2.0	2.0	2.0
Phenyl beta naphthylamine	1.0	1.0	1.0	1.0
Captax	0.75	0.75	0.75	0.70
Diphenyl guanidine	0.20	0.30	0.50	0.20
Sulfur	2.5	2.0	1.50	2.50
Butyl reclaim				60.0
Calcium silicate	10.0	10.0	10.0	
Total parts	191.45	191.05	190.75	241.40

Irradiation produces qualitative changes in Vulcollan of the same nature as those produced in Hycar PA-21. The physical properties of Vulcollan are listed in Table 16 along with those of Hycar PA-21. A more complete description of Hycar PA-21 is given in a recent quarterly report.[2] Vulcollan appears to be more radiation-resistant than Hycar in all respects. Although the tensile strength of Vulcollan decreases faster at the beginning, it retains more strength than the Hycar after long periods of irradiation. The fact that the tensile strength of Hycar has increased markedly for the longest irradiation period does not mean that it is recovering, but that it is on the verge of deteriorating completely. During this final stage of damage many materials become very hard and brittle, with a resultant increase in tensile strength. The hardness and elongation values for Vulcollan are considerably better than those for the Hycar after the longest irradiation period, and the electrical properties of Vulcollan have undergone almost no change, whereas the resistivity of the Hycar has decreased by a factor of 10^4.

There are similarities between the radiation-induced hardening of elastomers and the hardening process by which unvulcanized raw rubber crystallizes upon aging. In many of these materials it is found that irradiation hardens the material and increases the specific gravity. Since these changes often occur with no gas evolution,[3] it is supposed that the hardening and the increase in specific gravity may not be caused by chemical reaction. This may then be taken as evidence

[2] *Ibid.*, pp. 43 to 46.

[3] C. D. Bopp, O. Sisman, R. L. Towns, and W. E. Kirkland, *Solid State Division Quarterly Progress Report for Period Ending January 31, 1952*, ORNL-1261, p. 23.

Table 15

RADIATION-PRODUCED CHANGES IN PHYSICAL PROPERTIES OF NATURAL AND BUTYL RUBBER COMBINATIONS

	ELASTOMERS			
	Natural Rubber to Butyl, 50:50	Natural Rubber to Butyl, 25:75	Natural Rubber to Butyl, 10:90	Natural Rubber to Butyl Reclaim, 100:60
Irradiation exposure (10^{18} nvt)	0 0.25 0.60	0 0.25 0.60	0 0.25 0.60	0 0.25 0.60
Tensile strength (psi)	2100 800 400	1700 400 170	1600 200 Tarry	2000 900 500
Elongation (%)	315 65 40	230 70 30	205 110	375 115 30
Shore durometer hardness	69 72 74	69 64 60	70 52	63 71 79
Shore elasticity	77 50 35	83 30 25	80 30	90 60 35
Compression set (%)				
Strain immediately after application of load	30 – 20	28 – Too tarry to test	25 – Too tarry to test	25 – 14
Final deformation	10 – 19	6 –	5 –	8 – 3.8
Specific gravity (25°/6°C)	1.223 1.218 1.208	1.232 1.223 1.121	1.235 1.235 1.10	1.175 1.175 1.175
Change in weight (%)	-0.14	0.18	0.05	0.03
Volume resistivity (ohm-cm)	10^{10} 10^{10} 10^{10}	10^{10} 10^{10} 10^{10}	10^{12} 10^{13}	10^{8} 10^{9} 10^{9}
Dielectric strength (v/mil)	130 190 280	140 120 120	140 110	150 180 220

Table 16
COMPARISON OF RADIATION DAMAGE TO HYCAR PA-21 WITH THAT TO VULCOLLAN

	ELASTOMERS	
	Hycar PA-21	Vulcollan
Irradiation exposure (10^{18} nvt)	0	0
	0.25	0.25
	1.6	1.6
	5.4	5.4
Tensile strength (psi)	2000	5400
	1200	1890
	400	590
	1500	240
Elongation (%)	330	600
	80	250
	20	50
	<2	10
Shore durometer hardness	62	74
	82	72
	88	74
	99	90
Shore elasticity	70	100
	43	80
	25	30
	-	25
Specific gravity (25°/4°C)	1.269	1.237
	1.270	1.242
	1.276	1.245
	1.290	1.256
Change in weight (%)	-	-
	-0.17	0.05
	-1.7	-0.19
	-7.0	-5.8
Volume resistivity (ohm-cm)	10^{10}	3×10^{8}
	-	3×10^{8}
	-	3×10^{8}
	10^{6}	3×10^{8}
Dielectric strength (v/mil)	115	>210
	115	>210
	115	>210
	115	200

that the materials are becoming more crystalline. A program has been initiated to study the x-ray diffraction patterns (cf., "X-Ray Work," this report) of irradiated and non-irradiated elastomers to obtain additional data on the change in structure of these materials.

RADIATION-INDUCED ACTIVITY IN MATERIALS OF CONSTRUCTION

C. D. Bopp R. L. Towns
W. K. Kirkland

The gamma decay of several stainless steels and other alloys and metals that were activated in the isotope stringer of the ORNL graphite reactor has been observed long enough so that the major portion of the remaining activity is now Co^{60}. The quantity of cobalt is greatest for nickel-containing alloys, but an amount of the order of 0.01% is present in all the iron alloys. A report containing decay curves for all the materials irradiated is nearly complete and will probably be issued during the coming quarterly period.

A curve presented in ORNL-1095[4] as the decay of reactor-irradiated tungsten has been found to be in error. The material was tungsten steel, analyzed as 35.27% tungsten, 63.97% iron, 0.047% manganese, and less than 0.001% cobalt. In the future, spectrographic analyses will be made of all the materials for which decay curves are given.

[4] *Physics of Solids Institute Quarterly Progress Report for Period Ending April 30, 1951*, ORNL-1095, p. 86.

CRYSTAL PHYSICS

X-RAY WORK

G. E. Klein F. A. Sherrill

The North American Philips x-ray unit was installed and equipped with a high-voltage switch that enables the power from the Philips power supply to be switched instantaneously to the General Electric hot-cell spectrometer, to a second x-ray table containing a Philips high-angle spectrometer, or to the tube in the Philips unit itself. The high-voltage switch is equipped with interlocks and safeguards so that no damage to any equipment will result if the cooling water is not turned on or if accidental switching takes place on any of the units.

Because the high voltage must be transmitted to the G-E hot-cell spectrometer through approximately 70 ft of high-tension cable, and also since the G-E type CA-7 diffraction tube filament contains higher resistance than the filament in a Philips tube, the maximum current output obtainable from the G-E x-ray tube is approximately 7 ma, as compared with 20 ma from a Philips tube. This does not, however, prevent the radiation from the G-E tube from being usable for several types of experiments.

The hot-cell spectrometer is still located in the bench-test position outside of hot cell No. 3. It is being used to determine rocking-curve data from single crystals of copper. In this setup the x-ray beam impinges on a single crystal of mica, and the monochromatized beam is allowed to fall on a particular crystallographic plane of the copper crystal that is mounted on a goniometer head. The intensity of the diffracted beam is recorded in a proportional counter circuit. The plane of the copper crystal is next moved through accurately determined angles, and the corresponding intensity distribution is recorded for each point.

Work with the small-angle scattering equipment has involved minor modifications in this apparatus. The copper x-ray radiation is monochromatized by a calcite crystal to give a sharply defined beam of $Cu_{K\alpha_1 K\alpha_2}$ radiation that enters an evacuated chamber and passes through a vertical-slit system designed to cut out the $Cu_{K\alpha_2}$ component.

Patterns of elastomers and plastics before and after irradiation are being recorded to determine whether changes are produced in the structure of the various materials by bombardment. The results of the x-ray examination will be correlated with changes in engineering properties of the materials that have been observed. A library of x-ray patterns of many elastomers and plastics is being built up for future reference.

SPECIAL PROJECTS

RADIATION DAMAGE TO MISCELLANEOUS MATERIALS

R. H. Kernohan

Electrical resistivity measurements were made on two irradiated specimens of copper-gold alloy, one ordered and the other disordered. The specimens had been subjected to an nvt of 1.7×10^{20}. The resistivity, corrected to 0°C, of the disordered specimen had increased from 11.21 to 11.73 μohm-cm, whereas the resistivity of the ordered specimen had increased from 4.44 to 10.73 μohm-cm. This work may be correlated with work previously published on order-disorder phenomena in copper-gold samples.[1]

Rough measurements were made of the induced activity of a number of materials. These substances were weighed and placed in the center of hole B of the ORNL graphite reactor for approximately one week. The total irradiation time was 153 hours. The beta and gamma activities were measured by means of a cutie pie held in contact with each specimen. Results are tabulated in Table 17.

[1] D. S. Billington and S. Siegel, *Effect of Nuclear Reactor Radiation on Metals*, ANCD-2010.

Table 17

ACTIVITY MEASUREMENTS OF MATERIALS EXPOSED IN THE ORNL GRAPHITE REACTOR, HOLE B

MATERIAL	BETA AND GAMMA ACTIVITY* (mr/hr/g)				
	5 hr After Removal	10 hr After Removal	27 hr After Removal	50 hr After Removal	125 hr After Removal
Aluminum, 99.96%	115	100	65	44	23
Aluminum, 99.75%	320	210	85	33	2
Iron (Swedish)	125	75	45	39	34
Magnesium (Dowmetal No. 58135)	170	125	55	24	7
Amber	103	95	45	22	11
Bakelite	180	148	65	27	9
Neoprene S	5500	4300	2100	860	320
Neoprene Q	2100	1325	775	500	275
Neoprene W	2500	1500	925	575	385
Neoprene GN	3150	2200	1225	725	445
Neoprene KNR	2250	1825	925	600	375
Neoprene GNA	2650	1775	1200	650	400
Neoprene R+	2350	2000	1000	600	370

*Measurements made with cutie pie held in contact with specimen.